Faculty of Mechanical Engineering

Master of Science in Manufacturing Technology

Department of Materials Test Engineering

Prof. Dr.-Ing. habil. Frank Walther

Investigation of weld quality for friction stir welding of extruded 6000 series aluminum alloys

Master Thesis

Name: Ezgi Yagmur Keskin

Matriculation No.: 198552

Supervisor: Prof. Dr. –Ing. habil.Frank Walther
Assist. Prof. Dr. Mehmet Ipekoglu
M.Sc. Mustafa Awd

Submission date: 16 September 2019

26.09.2019

The result of the thesis presentation of Ezgi Yağmur KESKİN, who is registered in the joint graduate program Manufacturing Technology between Turkish-German University and Technical University Dortmund with the registration number 1661011105, titled "Investigation of Weld Quality for Friction Stir Welding of Extruded 6000 Series Aluminum Alloys" held on 26.09.2019 at 14:00 is presented below.

| ✓ | Successful | | Extension (3 months) | | Unsuccessful |

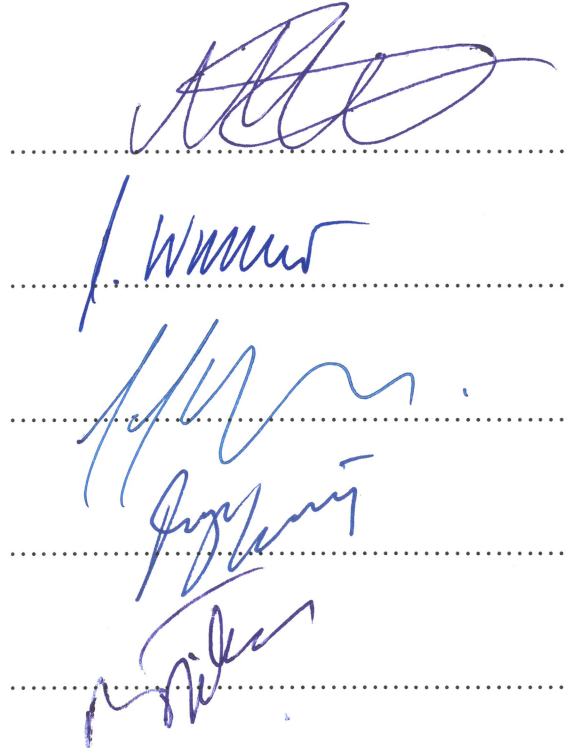Thesis Presentation Committee:

Dr. Mehmet İPEKOĞLU
(Advisor)

Prof. Dr.-Ing. Frank WALTHER
(Co-advisor)

Assoc. Prof. Dr. Güney Güven YAPICI
(Member)

Dr. Duygu EKİNCİ
(Member)

Dr. Mehmet Gökhan GÖKÇEN
(Member)

Eidesstattliche Versicherung
(Affidavit)

Keskin, Ezgi Yagmur
Name, Vorname
(Last name, first name)

198552
Matrikelnr.
(Enrollment number)

Titel der Bachelor-/Masterarbeit*:
(Title of the Bachelor's/ Master's* thesis):

Investigation of weld quality for friction stir welding of extruded 6000 series aluminum alloys

*Nichtzutreffendes bitte streichen
(Please choose the appropriate)

Istanbul, 16.09.2019
Ort, Datum
(Place, date)

UKeskin
Unterschrift
(Signature)

Istanbul, 16.09.2019
Ort, Datum
(Place, date)

UKeskin
Unterschrift
(Signature)

technische universität
dortmund

TÜRK-ALMAN ÜNİVERSİTESİ
TÜRKISCH-DEUTSCHE UNIVERSITÄT

Master's Thesis

wpt Werkstoffprüftechnik
Prof. Dr.-Ing. habil. Frank Walther
www.wpt-info.de

Name:	**Ezgi Yagmur Keskin**
Supervisors:	**Prof. Dr. –Ing. habil.Frank Walther, Assist. Prof. Dr. Mehmet Ipekoglu, M.Sc. Mustafa Awd**
Subject:	**Investigation of weld quality for friction stir welding of extruded 6000 series aluminum alloys**

Aluminum alloys are preferred in various industries such as in transportation industry including automotive, marine, and rail transport in various structural parts and several components since they have many advantageous properties like good strength-to-weight ratio and good corrosion resistance, improved fatigue strength among other materials. Joining especially welding is usually required in many applications; however, fusion welding as a mostly-applied welding technique is problematic when it is applied to aluminum alloys. For this reason, other joining techniques are needed to be developed. Friction stir welding is a relatively new joining technique providing many advantages among other joining processes. This process accomplishes the joining of aluminum alloys, and dissimilar material successfully.

In this study, the welding behavior of 6000 series aluminum alloys were investigated by joining AA 6005 and AA 6082 alloys. In total, three different sets were included in the test plan: Welding of AA 6082 to AA 6082; welding of AA 6005 to AA 6005, and welding of AA 6005 to AA 6082. The main process parameters in this study were rotational speed and welding speed. The 5-axis CNC machine was adopted to perform welding with a designed taper threaded friction stir tool. The special fixture were designed and manufactured for a safe welding process.

Weld quality was examined with several tests including tensile test, microhardness test, microscopic and macroscopic analyses. The results were presented and the relationships between welding parameters and resultant joint properties were investigated.

This study was conducted in ASAŞ Alüminyum Sanayi ve Ticaret A.Ş.in Sakarya, Turkey.

Dortmund, 16 September 2019

(Prof. Dr.-Ing. habil. Frank Walther)

Table of Content

Abbreviations and Symbols

Abbreviation	Designation
Al	Aluminum
SEM	Scanning electron microscope
FSW	Friction stir welding
HAZ	Heat-affected zone
TMAZ	Thermo-mechanically affected zone
SZ	Stir zone
BM	Base metal
PM	Parent metal
HV	Vickers Hardness
HRC	Rockwell Hardness
AS	Advancing side
RS	Retreating side
EDS	Energy Dispersive X-ray Spectroscopy

Symbols	Unit	Designation
$\sigma_{base\ metal}$	MPa	Tensile strength of base metal
σ_{joint}	MPa	Tensile strength of the joint
$\sigma_{min,w}$	MPa	Required minimum tensile strength
$\sigma_{min,pm}$	MPa	Minimum tensile strength of the base metal
f_e	-	Efficiency of the connection

1 Introduction

Aluminum alloys are highly demanded materials in many industrial areas including automotive, architecture, aerospace, and marine and shipbuilding industries due to their valuable properties such as their strength values relative to their low density, improved fatigue strength, and high corrosion resistance. Also, their highly formable aspect makes them irreplaceable in the industry.

In several applications, joining techniques such as adhesive bonding, mechanical fastening, and welding are needed to be performed in order to manage the whole working system while it is not possible to manufacture big and complex components at once. Each of the joining techniques has their own advantages and disadvantages; welding process has also many limitations and drawbacks; nonetheless, it is almost inevitable in many industries such as marine and aerospace industries to join the immense plates together. Fusion welding is highly applied welding techniques where the materials to be welded are fused together, reaching the melting point. Even though it is highly applicable and gives successful results for steel, it is not desired technique for aluminum alloys due to many problematic reactions of the aluminum alloys to fusion welding process. Aluminum alloys are usually considered as non-weldable since they have poor microstructure in solidification and porosity in the fusion region; moreover, mechanical properties in the joint in comparison with base metal cannot be overlooked [Pra13]. Resistance welding can be applied some of the aluminum alloys; however, oxide on surface is a great problem, and preparation of the surface is expensive [Pra13]. For fusion welding, liquation cracking and hydrogen embrittlement may not be entirely eliminated for the majority of the welded joint of aluminum alloys; even many precautions are taken; therefore, solid-state welding processes are more convenient due to the exclusion of total melting and fusion related problems [Ven13]. As a result, friction stir welding (FSW) process is highly preferable relatively new technology for welding of aluminum alloys. FSW process has many advantages over fusion welding since it does not involve melting of the parent metal. It is even applicable for the most difficult-to-weld aluminum alloys such as 7xxx series aluminum alloys. FSW provides better stability in dimension, low residual stresses and better reservation of the parent metal properties [Jat00]. FSW is also environmentally friendly process, which eliminates the need for varied gases that commonly accompany conventional fusion welding [Jat00].

Joining dissimilar aluminum alloys is another complex tasks for conventional fusion welding processes since reduced strength and integrity in a structure may occur easily as a consequence of the difference in mechanical, thermal, and metallurgical properties causing difficulty in mixing of the material and imbalance in solidification [Kha17]. Another significant aspect of FSW process is that it allows the welding of dissimilar welding, which makes FSW

outstanding among other welding processes. Joining of dissimilar welding is a complicated task for several reasons; for example, the selection of proper filler material in fusion welding is crucial since inappropriate selection may cause formation of brittle intermetallic compounds, which corrupt the quality of the weld; solid-state welding also may create not only compatibility problems resulting from different physical properties of dissimilar materials but also formation of intermetallic compounds [Kum12].

Friction stir welding process is a solid-state welding process which uses non-consumable, rotating tool to regionally soften the material through developed heat as a result of plastic deformation and friction. Also, FSW tool is allowed to stir the surfaces of the joint [Loh10]. FSW was firstly invented by Wayne Thomas and his colleagues from The Welding Institute (TWI) in 1991 [Kha17].

Many researchers have indicated that FSW creates sound and desires joining properties for many combinations of different materials including steels and aluminum alloys. In this study, the main aim is to examine the behavior of 6000 series aluminum alloys in both similar and dissimilar welding to FSW process; for this purpose, AA 6005-T6 and AA 6082-T6 extruded aluminum plates were utilized. Two of the main parameters were analyzed with emphasis: Rotational speed and welding speed. According to test results showing the quality of the weld joint, the best optimum parameters for the decided sets of parameters are tried to be found; moreover, effect of the parameters on the mechanical and microstructural properties was tried to be understood.

The detailed knowledge of the process was explained in the following sections throughout the study.

2 State of the Art

2.1 Aluminum Alloys

Aluminum alloys are greatly utilized in several industries such as shipbuilding, marine, aerospace, and rail transport in various structural parts and several components thanks to their numerous desirable properties like great strength-to-weight ratio, improved fatigue strength and good corrosion resistance [Kha17]. Especially in the transportation and manufacturing area, an increase in the use of aluminum is predicted to continue all around the world [Kha17]. For commercial and military aircraft for nearly 80 years, lightweight aluminum alloys have been the main structural material because of their good mechanical behavior and developed manufacturing processes, and they will reserve their place with developing new-generation high strength aluminum alloys [Kha17]. Even though the greatest use of Aluminum alloys was reported by European Aluminum to be in the transportation sector, packaging sector follows transportation with rapid development speed [Dog 06]; [Mal10].

In the transportation industry, fuel consumption and harmful emissions are decreased by the use of light-weight material such as aluminum alloys [Kha17].

Unlike steel which experiences phase changes or crystal transformation at particular temperatures, aluminum does not alter its crystal structure on cooling or heating. This enables the steel to harden by rapid cooling; however, aluminum alloys are affected little or not by the changes in cooling rate [Mat02]. They have different hardening mechanisms as they will be introduced further in the text.

Aluminum alloys can be divided into two main categories: Wrought and cast aluminum alloys. Further classification is made based on the basic method of property development for each category [Dav01]. Various alloys react to thermal treatment, including age hardening, quenching, and solution heat treatment, depending on phase solubility [Dav01]. Those alloys, either casting or wrought alloys, are named as heat treatable [Dav01]. Many other wrought alloys, which are described as non-heat treatable alloys, are strengthened by work hardening with annealing procedure. The non-heat treatable casting alloys are used solely in as-cast or in thermally modified states unrelated precipitation or solution effects [Dav01]. Table 2.1 states the designation system by Aluminum Association for both casting and wrought aluminum alloys.

Table 2.1: Aluminum alloys and their alloying elements [Kau00]

Aluminum Alloys

Casting alloys	Alloying elements	Wrought alloys	Main alloying element
1xx.x	Unalloyed	1xxx	Mostly pure aluminum
2xx.x	Copper	2xxx	Copper
3xx.x	Silicon plus copper and/or magnesium	3xxx	Manganese
4xx.x	Silicon	4xxx	Silicon
5xx.x	Magnesium	5xxx	Magnesium
6xx.x	Not used	6xxx	Magnesium and Silicon
7xx.x	Zinc	7xxx	Zinc
8xx.x	Tin	8xxx	Other elements
9xx.x	Other elements	9xxx	Unassigned

Aluminum alloys are categorized as heat-treatable or non-heat treatable based on their response to precipitation hardening. 2xxx with copper, 6xxx with magnesium silicide(Mg2Si) and 7xxx with zinc content are heat treatable wrought alloys and strengthened by precipitation hardening. 1xxx, pure aluminum, 3xxx with manganese, and 5xxx with magnesium content are non-heat treatable alloys [Dag16].

Wrought aluminum alloys with their major alloying element, typical composition, typical properties, and applications are listed in Table 2.2.

Table 2.2: Typical composition, properties, and application of aluminum alloys [Kha17]

Aluminum alloys	Typical composition (wt. %)	Typical Properties and application
1xx.x	>99 Al	Good electrical conductor, low strength: cooking foil, power transmission, utensils
2xx.x	Al + 4–6 Cu + Mg	Strong heat-treatable alloy: aircraft external tanks, lower wings, fuselage
3xx.x	Al + Mn	Medium strength, excellent corrosion resistance, ductile: beverage cans, roofing, cooking pans, automotive radiators
5xx.x	Al + 3 Mg	Strong work hardening alloy: pressure vessel, ship hulls, inner automotive body panel, boilers, storage tanks
6xx.x	Al + Mg + Si	Moderate strength heat-treatable alloy: pipelines, bridges, external automotive body panel, structural members
7xx.x	Al + 6 Zn + 2 Mg + 1.5 Cu	Strong heat-treatable alloy: aircraft upper wings, fuselage
Al-Li alloys	Al + 3 Li	Good strength to weight and low density: aircraft spar and skins

2.1.1 6XXX Aluminum Alloys

In this study, 6xxx aluminum alloys are the main focus for the friction stir welding process. In ASAŞ Aluminum Company, various forms of 6xxx alloys are manufactured with diverse manufacturing methods including extrusion and rolling.

Main alloying elements in 6xxx are magnesium and silicon. They have excellent precipitation hardening capability as they construct a quasi-binary section with Mg_2Si phase of the magnesium-silicon system. This capability also provides 6xxx alloys moderately higher strengths compared to non-heat treatable alloys, generally with a combination of great corrosion resistance [Kau00].

As alloying elements in 6xxx series alloys; Magnesium (Mg) provides improved work hardening ability and through solid solution strengthening increased strength; Silicon (Si) improves ductility and strength, together with magnesium generates precipitation hardening [Mat02].

6xxx alloys are one of the easiest among aluminum alloys to extrude and broadly preferred for complex shapes manufactured in this way. Moreover, with nearly all commercial processes, they are easily joined [Kau00].

This series of heat-treatable alloys can be formed in T4 temper and by precipitation heat treatment can be strengthened to full T6 properties after forming [Dav01]. While T4 temper includes solution heat treatment and natural aging to substantially stable condition, T6 temper refers to solution heat-treated and artificially aged condition [Dag16].

2.2   Joining Techniques for Aluminum Alloys

In many industrial applications, components are often needed to be joined in order to produce a designed whole part. Those subcomponents to be joined may be made of either similar or dissimilar materials.

Even though the number and length of the needed structural and non-structural joints are reduced considerably through a designation of large, integrated aluminum parts like single-piece sheet deep drawings, and extrusion with sophisticated cross-sections, for aluminum structures and mixed material designs, reliable and consistent joining methods are still needed [Eaa17].

Primarily, there are three main principles for material joining as stated at Aluminum Automotive Manual by European Aluminum Association [Eaa15]:

- Material coalescence: Molecular or atomic forces hold materials together; thus, atoms and/or molecules must be placed very close to each other, e.g. by processes based upon the mixing in liquid state as fusion welding or processes excluding the presence of heat such as diffusion or solid-state welding or processes containing a third liquid material like adhesive bonding or soldering.
- Friction connections: This joining technique is achieved as a result of friction between the participating materials, reinforced by the application of an external load, e.g. shrinking of a hub onto the shaft.
- Interlocking joints: They are created by the interlocking of two materials or by the anchoring of the added components inside or into the corresponding parts, i.e. mechanical joints.

Adhesive bonding, welding, mechanical fasting, soldering, clinching, brazing, and injected metal assembly are among various joining techniques used to join similar and dissimilar materials, as shown in Figure 2.2 [Kum15].
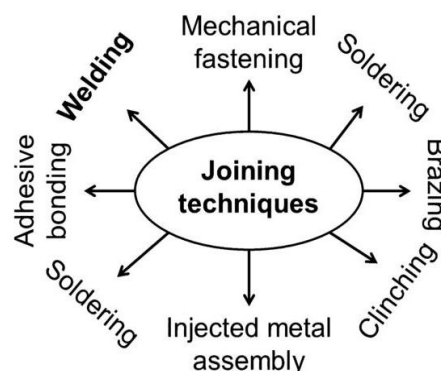
Figure 2.1: Various joining techniques for joining of similar and dissimilar materials [Kum15]

For the manufacturing of several components of aircraft and ships, mechanical fastening like screwing, riveting is used traditionally, also occasionally arc welding is applied [Kha17]. Nonetheless, mechanical fastening has several drawbacks; extra operations such as creating a hole and clamping are required for accomplishing fit-up, joints are sensitive to corrosion, and internal joints are rather difficult to make [Kha17]. As cited by Khan& Khan [Kha17], Barnes and Pashby stated that those joints in a corrosive medium serve as crack initiation region, and degrade the joint strength significantly [Bar00].

As indicated in Figure 2.1, there are various techniques for joining; nevertheless, among all, welding steps forward with its many advantages. It provides flexible design, faster integration time, increased structural stiffness, and savings in weight, high joint efficiency, water, and air tightness, no limitation on the width of the parts to e welded together [Kum15].
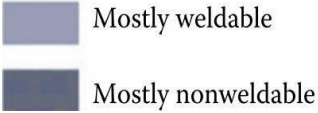
The description of the welding can be made as to the joining of the two parts by a coalescence of the adjacent surfaces. If this coalescence is managed with melting of the two parts together, it is called as fusion welding, if it is achieved by joining the two parts together under pressure, with or without applying heat simultaneously, to create a metallic bond at the interface, it is named as solid-phase joining. Also, more modern solid-phase methods are represented as friction welding [Mat02]. Friction welding, explosive welding, ultrasonic welding, cold and hot pressure welding are among the solid-phase bonding processes.

The suitability of an aluminum part for welding is described as weldability, and it depends on the following factors [Eaa15]:

- Quality of base material, including surface properties, alloy composition, etc.
- Design, i.e. joint design, design suitability for welding, etc.
- Welding process including welding processing parameters, welding method, and equipment, etc.

Fusion welding is among the most frequently applied joining technique for aluminum alloys; however, there are some aluminum alloys referred as "non-weldable" as a result of their problematic behavior in welded condition, namely high tendency to solidification cracking and also increased sensitivity to stress corrosion cracking [Eaa15]. 2xxx and 7xxx series aluminum alloys are listed as non-weldable alloys for fusion welding process, as shown in Figure 2.2 since there is loss in mechanical properties in comparison with base metal for this welds, they also have porosity in the fusion zone and weak solidification microstructure [Mis05]. It can be seen that there is another welding technique which enables welding of most of the aluminum alloy series including 2xxx and 7xxx, named as friction stir welding.

	1XXX	2XXX	3XXX	4XXX	5XXX	6XXX	7XXX	8XXX
Commercial welding								
Friction stir welding								

Mostly weldable

Mostly nonweldable

Figure 2.2: Weldability of aluminum alloys by conventional and FSW process [Kha17]

2.2.1 Fusion Welding of Aluminum Alloys

Fusion welding is distinguished by melting of workpieces partially to form a pool of molten metal which by subsequent cooling solidifies and results in a firm joint, and in order to produce the weld, different sources of energy including electricity, friction, laser and electron beam are utilized [Eaa15].

Material A   Material B

Parent metal   Fusion zone   Transition zone   Heat affected zone
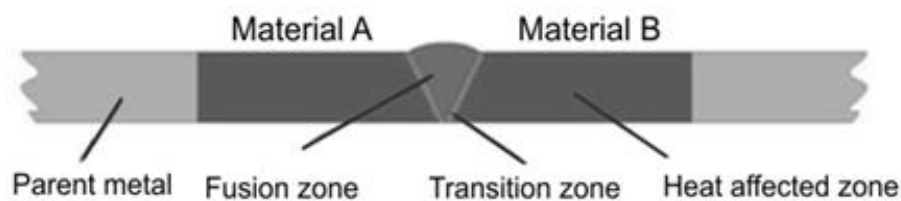
Figure 2.3: Characteristics of the welding zone in fusion welding

In Figure 2.3, the characteristic welding zone for fusion welding is stated illustrating three distinctive zones: fusion zone, transition zone, and heat-affected zone. In the fusion zone, the molten metal from both A and B materials are present, also if applicable filler metal is involved in the melt. In the transition zone, the eutectic phases at the grain boundaries melt, also along the grain boundaries; diffusion of the alloying elements will take place. In the heat-affected zone, depending on the reached level of temperature, thermally governed solid-state processes such as precipitation, recrystallization, and recovery processes, and segregation effects may occur [Eaa15].

Fusion welding techniques can be conducted either without filler materials, which is named as autogenous welding or with filler metal, which is more frequently applied. Filler metal, forming together with the melted parent material the weld metal, can be introduced in the form of a rod or wire and melted into the joint [Mat02].

Heat source directed at joint area should be intense enough to generate a rapid fusion of the metal (and filler) to be welded for fusion welding. Heat sources used most frequently are light (laser), electron bombardment, flame, and most of all the electric arc [Cor88].

Most frequently applied fusion welding methods according to the heat sources used can be listed in three categories: Gas welding, arc welding, and power beam processes. Metal arc welding and gas shielded arc welding are included in arc welding category whereas laser welding and electron beam welding are parts power beam processes [Wem03].

Power beam processes include laser and electron beam welding. Laser and electron beams supply a localized high density of power, enabling narrow, deep penetration welds and high speeds in welding with minimum power input. Low residual stresses, small heat-affected zones, and decreased geometrical distortions are obtained as a result of localized heat input. Moreover, robotic or mechanized systems are applicable to structural power beam processes [Eaa17].

In gas welding, the combustion of acetylene in oxygen generates heat; the temperature of the generated flame is less than the temperature of an electric arc, the heat is also less condensed. In Figure 2.4, a gas set, including acetylene and oxygen is shown. Depending on their chemical impact on the melt pool, there are three different kinds of flames: Carburizing, oxidizing and neutral. Neutral flame, which is mostly used in gas welding, is illustrated in Figure 2.5 indicating the zones of the flame. The flame is pointed onto the joint surfaces, which melt, after which filler material can be fed as necessary. The reducing zone and the outer zone of the flame, as illustrated in Figure 2.5, protect the melt pool from the air; thus, the flame should be taken away slowly when the weld is accomplished. Gas welding is mainly used for repair and erection work and is less commonly applied today [Wem03].

**Figure 2.4:** A gas welding set [Wem03]

$$C_2H_2 + O_2 = 2CO + H_2$$
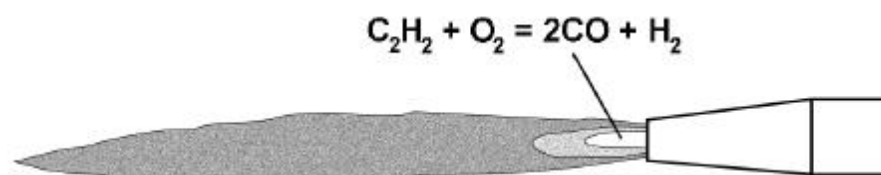
Figure 2.5: A neutral gas flame with the innermost reaction zone, reducing zone in the middle and outer zone where combustion continues with oxygen from surrounding air [Wem03]

An electric arc is one of the most frequently used heat source in fusion welding. It is generated by an electric discharge between the workpieces to be joined and an electrode producing sufficient heat to melt the metal under the arc. The weld is formed through the solidification of the melted material. Consumable and non-consumable electrodes can be utilized in arc welding processes. In the first condition, the molten base material mixes together with the fused metal from the electrode, and a joint is formed by solidification upon cooling, a flux or a shielding gas is applied in order to insulate the molten material from the surrounding atmosphere or contamination. In the second condition, the joint is composed of base metal that melts and solidifies [Qui12].

Parts of the arc welding processes are shielded metal arc welding (SMAW), gas tungsten arc welding (GTAW), gas metal arc welding (GMAW), and submerged arc welding (SAW).

Some of the most commonly applied fusion welding techniques to aluminum alloys are MIG/MAG/GMAW (Metal Inert Gas/Metal Active Gas/Gas Metal Arc Welding), TIG/GTAW (Tungsten Inert Gas/Gas Tungsten Arc Welding), and Oxygas welding [Qui12].

Gas tungsten arc welding (GTAW)/ Tungsten Inert Gas Welding (TIG) is illustrated in Figure 2.6, the process utilizes an electric arc between the metal to be welded, and a non-consumable tungsten electrode and inert shielding gas protect the melt from the contamination in the atmosphere [Qui12].
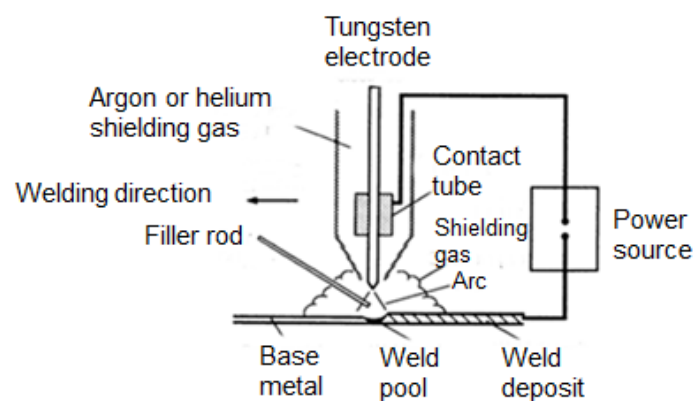
Figure 2.6: Gas tungsten arc welding (GTAW) [Kou87]

In metal inert gas welding (MIG) as shown in Figure 2.7, a wire both as filler material and as the electrode is continuously fed, and an inert gas shield protects the weld pool and the arc. It provides the benefits of narrower heat-affected zones, increased welding speeds than TIG welding, perfect removal of oxide film during welding and welding capability in all positions. MIG welding is for these reasons most widely used manual arc welding technique for aluminum joining [Mat02].
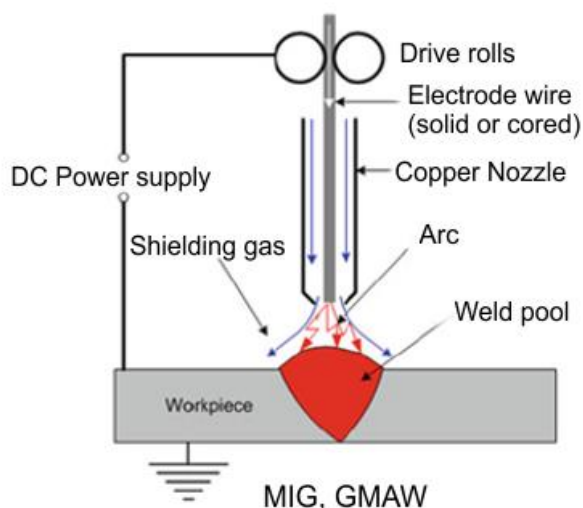
Figure 2.7: Metal inert gas welding (MIG) [Qui12]

2.2.2 Problems of Fusion Welding

In conventional fusion welding processes, melting of base metal takes place; this generates many problems causing unfavorable solidification microstructure and joint quality [Kha17]. Moreover, various pre-welding processes applied to workpieces in fusion welding causes the properties of base metal to deteriorate, especially in the welded zone and the material nearby [Kha17]. As cited by Khan and Khan [Kha17], Su and his colleagues [Su03] stated that joint's mechanical properties are negatively affected by brittle interdendritic structure, which is a result of melting and solidification of the fusion zone of the weld.

Fusion welding processes is especially more difficult for aluminum alloys in comparison with steel since due to the high thermal conductivity of aluminum alloys; they need high heat input. Also, their high affinity to oxygen requires proper shielding gas in fusion welding. In order to obtain high heat input, high temperatures are necessary, which will enlarge the heat-affected zone (HAZ), leading to a significant decrease in the joint quality. Moreover, the mechanical properties of the workpiece are degraded at high heat inputs for age hardenable aluminum alloys(2xxx, 6xxx, 7xxx) by precipitation dissolution, for strain hardenable aluminum alloys (5xxx) by loss of cold work [Kha17]. Several welding defects like solidification cracking, weld distortion, and porosity are formed at comparatively higher temperatures [Kha17].

Malyer [Mal10] has cited that high heat input in arc welding, particularly for age hardenable aluminum alloys being more sensitive to cracks, high thermal expansion, large solidification range, and creation of phases with low solidus temperature at the grain boundaries of the heat-affected zone of the strengthened aluminum alloys cause crack formation [Ata03].

In the molten weld metal, some gases may dissolve and as the melt solidifies these gases may trap in the solidified weld, creating bubbles. This problem is named as porosity [Mat02]. In aluminum alloys, hydrogen causes porosity problem, the reason is that hydrogen is highly

soluble in molten aluminum whereas it has low solubility in the solidified weld as illustrated in Figure 2.8 [Mat02].
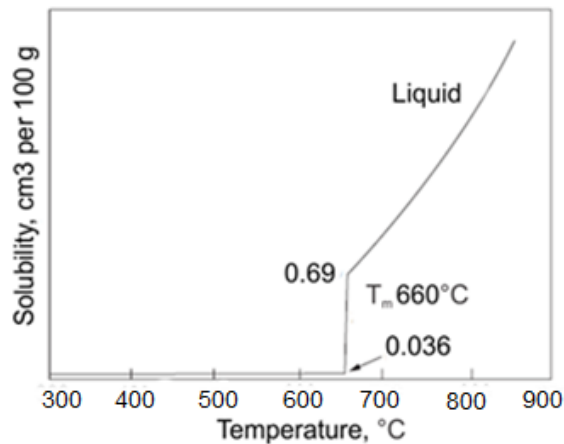
**Figure 2.8:** Solubility of hydrogen in aluminum [Mat02]

One of the main sources of the hydrogen is the welding consumables. For instance, the flux shielded processes including manual metallic arc (MMA) or shielded metal arc welding (SMA) welding are not commonly applied to weld aluminum since the flux has moisture as its intrinsic part, and during welding this causes very porous welding zone by hydrogen forming through the decomposition of the moisture in the arc. Moreover, for accomplishing the low amount of porosity, the parent metal must be cleaned very carefully by various methods including degreasing, and stainless steel wire brushing [Mat02].

Aluminum oxide (Al_2O_3) will be formed at the surface when aluminum is heated in an open atmosphere since it is highly reactive towards oxygen, Al_2O_3 can also be formed in fusion welding processes, and cause problems in the weld. Al_2O_3 has a very higher melting temperature (approximately 2000°C) and higher density as compared to aluminum (660°C), and it prevents the bonding of molten aluminum particles, which is required for a successful welding process. Also, the heat required for melting the oxide layer may results in excessive melting of the aluminum alloy [Yav97], [Mal10]. In order to prevent defects like oxide film entrapment and lack of fusion, the oxide film layer is needed to be dispersed during welding [Mat02].

Fusion welding of the aluminum is prone to distortion of the welded workpieces, aluminum requires locally intense heat input for welding due to its high thermal conductivity, and it has also high thermal expansion coefficient, which altogether leads to large deformations, and accordingly high internal stresses. Therefore, fusion welding is needed to be done at high welding speeds in order to minimize distortion [Mal10].

Hot cracking, also named as solidification cracking, is another problem occurred in the fusion welding of certain alloy systems. During the last stages of the solidification of the metal, a

liquid having low melting point surrounds the grain boundaries of the solid phase, the larger the difference in the melting temperature between the liquid film having a low melting point and the metal bulk is, the more sensitive the weld will be towards hot cracking. Aluminum alloys have deliberately added alloying elements were forming a range of eutectics with highly lower freezing temperatures than the bulk metal, which means that all aluminum alloys are somewhat prone to this type of cracking with varying degree of the crack sensitivity [Mat02]. The effect of some solute concentrations for aluminum is shown in Figure 2.9.
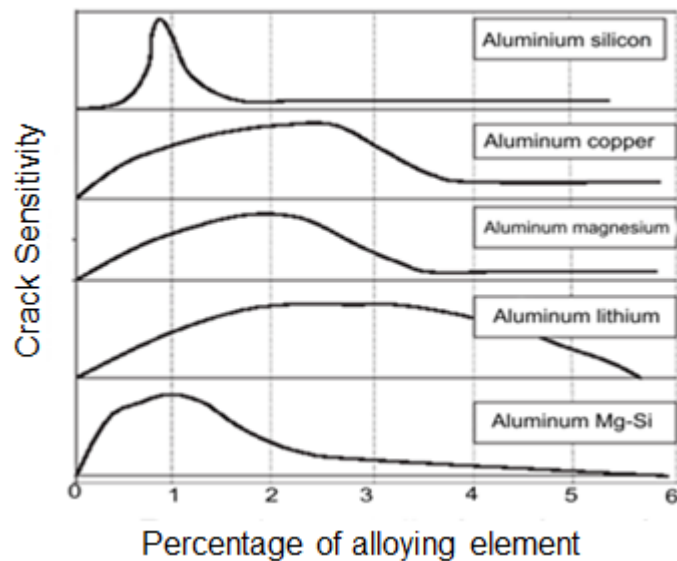
Figure 2.9: Effect of some solute concentrations on crack sensitivity [Mat02]

As cited by Khan and Khan [Kha17], Barnes and Pashby [Bar00] stated that aluminum alloys could be welded by several fusion welding techniques including high energy electron beam welding (EBW), resistance spot welding (RSW), and high energy laser beam welding (LBW); nonetheless, there are various disadvantages regarding these processes in technical and economical way such as costly capital investment, mismatch in joint line in LBW, electrode wear in RSW, etc., which promote to use some other welding techniques instead of these processes.

Some problems regarding the fusion welding of aluminum alloys such as hot cracking and hydrogen embrittlement may not be entirely prevented in most cases; therefore, solid-state welding of aluminum alloys steps forward as it excludes the melting of the alloy during the process. As a solid-state welding process, friction stir welding has great advantages over the fusion welding for the aluminum alloys [Ven13].

In friction stir welding (FSW), elimination of the complete melting of the aluminum alloys provides problem-free welding in terms of solidification-related cracking and porosities with low distortion. Moreover, the need for protective gases is eliminated in FSW of the aluminum alloys, in addition to this; exclusion of the formation of the fumes and arc-related emissions

from welding process makes FSW an environmentally friendly welding technique [Loh10].FSW is also known to be "green" technology thanks to its environment friendliness, energy efficiency, and versatility; it needs remarkably less energy [Mis05].

Friction stir welding does not use filler material; this eliminates the formation of the undesired phase resulting from the mixing of the parent and the filler metal in the microstructure of the weld [Loh10]. Moreover, a problem arising from the composition compatibility in fusion welding with filler metal is overcome by FSW [Mis05].
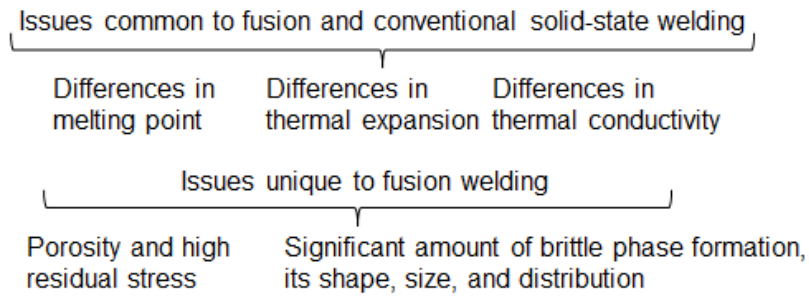
As discussed above, the melting in fusion welding creates many difficulties, including volumetric changes, changes in solubility of the gases, which arise from a state change during the process. These difficulties are avoided when the heat source is changed to plastic work and friction as in the friction stir welding [Loh10]. Less distortion and reduced residual stresses achieved by lower welding temperature provide increased fatigue performance, ability to weld very thick and thin plates, and new techniques for construction [Loh10]. FSW is a mostly fully automated technique with higher equipment cost; however, reduced operator skill than the arc welding processes. Moreover, FSW is not affected by the gravitation, allowing it to be applied in any orientation. FSW is a successful joining technique for the manufacturing area with several environmental, technical, and economic advantages over conventional fusion welding processes [Loh10].

2.2.3 Welding of Dissimilar Metals

Fusion welding of the dissimilar metals is highly challenging since the process includes melting of the base metal and for different aluminum alloys, thermal properties such as melting point and thermal conductivity considerably changes due to their major alloying elements, which makes the problematic fusion welding much more difficult [Kha17].

For the dissimilar metals, another problem in the fusion welding is the selection of the filler material since it is decided with regard to base metal, in most cases filler metal generates a weld metal with entirely different mechanical, physical and metallurgical properties than the each of the constituent dissimilar metals [Kha17], [Kum15].

In Figure 2.10, some of the problems encountered in fusion welding of dissimilar metal welding are illustrated. In most cases, hydrogen embrittlement, hot cracking due to dissimilar thermal properties and formation of hard and brittle intermetallic compounds which arises from varied metallic alloying elements in the alloy generates problems in dissimilar metal welding [Kha17].

Issues common to fusion and conventional solid-state welding

Differences in melting point

Differences in thermal expansion

Differences in thermal conductivity

Issues unique to fusion welding

Porosity and high residual stress

Significant amount of brittle phase formation, its shape, size, and distribution

Figure 2.10: Problems of dissimilar fusion welding [Kum15]

In FSW, severe shear forces on the material around the tool and temperatures below the melting point contribute reasonably to the welding of the dissimilar metals [Kum15]. In the literature, there are many successful examples of dissimilar metal welding by FSW.

2.3 Friction Stir Welding of Aluminum Alloys

Wayne Thomas and his colleagues from The Welding Institute (TWI) invented the solid-state joining technique FSW in 1991 [Kha17]. In FSW, a rotating, non-consumable tool having a special design of pin and shoulder is plunged into the adjacent edges of the workpieces to be joined until the tool shoulder touches the surface of the base metal and moves forward along the joint line [Mis05].

FSW has the terms friction and stir, coming from the working principle of the process. The term friction arises from the heat source of the process; in order to soften the base metal, frictional heat is required. The term stir emphasizes the material movement in the plastic deformation form. Sound welds are produced through the combination of heat softening the BM and meanwhile, plastic deformation mixing the BM [Kha17].

There are several successful applications of the FSW in the industry, providing various benefits among other joining techniques, which leads to increasing demand in the process. For instance, in the late 1990s, Eclipse Aviation has replaced their 70% of rivets in the main assembly of Eclipse 500 jets with the FSW through welding of 2024, 7075, or dissimilar 2024 to 7075 alloys. This replacement provides the company with an increased production rate, four aircraft per day [Loh10].

2.3.1 Basics of FSW

As explained earlier, FSW is accomplished with the specially designed tool with pin and shoulder having particular tasks during the process. The technique is illustrated in Figure 2.11.
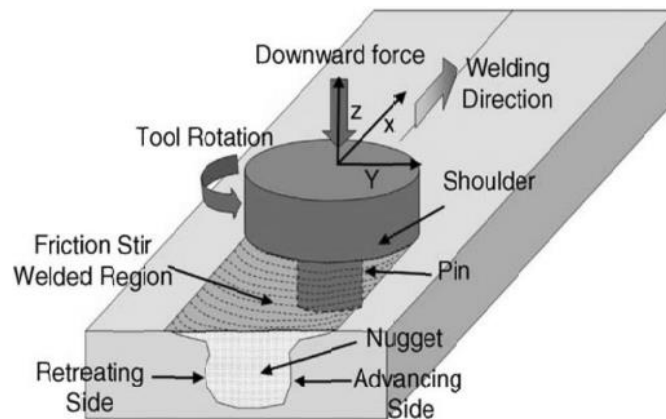
Figure 2.11: Terminology in FSW [Mis05]

Conventional FSW process consists of three distinct steps: Tool plunge, dwell period, and welding. In tool plunge, a rotating tool pin is forced into the joint of the plates o be welded till the tool shoulder touches the surfaces of the workpiece, in next step, which is dwell period, the tool rotates in the joint; however, does not traverse, with the purpose of initial heat generation for the plasticization of the material. After that, the rotating tool starts to move forward along the joint line and complete welding [Ull17]. The rotating tool is retracted after completion of the welding, leaving a keyhole at the end.

Main sources of the heat in FSW can be listed as follows: (i) friction arising from the contact between a non-consumable rotating tool and workpiece and (ii) plastic deformation of the workpiece material to be joined together [Kha17]. As cited by Lohwasser and Chen [Loh10], both Dong et al. [Don01], and Song and Kovecevic [Son03] decidedly suggest that heating resulting from plastic deformation is important and dominant in the lower region of the weld whereas frictional heat is dominant in the upper part of the stir zone.

Joining of the two plates is accomplished by that material travel around the tool from the front to the back of the tool by the effect of the feed motion and the tool rotation [Kum15]. Material flows from advancing side (AS) to retreating side (RS) of the tool and by forging effect of the tool shoulder; it is eventually consolidated at the back of the tool pin, and the joint is completed [Kha17].

In order to clarify advancing and retreating side orientations, rotation of the tool, and the direction of the travel must be known. In the advancing side, the directions of the tool rotation and welding are the same whereas, in the retreating side, the directions are opposite [Mis07].

Welding parameters, together with the design of the tool pin and the materials, govern the heated metal volume, softened metal moves around the tool in the rotation direction and is accumulated in the wake of the weld [Mis07].

In FSW, there are two crucial components in the process: Material flow and heat generation. These two elements govern the temperature history of the workpiece and contribute to flow

pattern and generated microstructure [Kum15]. Material flow phenomena in FSW is quite complex, and the knowledge of the deformation process is restricted. Material flow can be affected during FSW by various factors including welding parameters such as tool rotation rate and orientation; types of material; workpiece temperature; the geometry of the tool, etc. [Mis05].

2.3.2 Welding Zones

Welding zones formed by FSW is slightly different from the fusion welding process. There are two different classifications for the welding zone of FSW, one is made by Threadgill [Thr97] based on the microstructure of the weld, and the other is made by Arbegast [Arb03] based on the processing history in the weld zone [Kha17].

Arbegast asserted that there are close similarities between the microstructure of the typically hot worked aluminum by extrusion and forging, and the material flow properties and microstructure of the weld generated in FSW. Consequently, the FSW technique can be represented as a metalworking process with regard to five conventional zones of metalworking: (1) preheat, (2) initial deformation, (3) extrusion, (4) forging, and (5) post-heat/cool down zone [Mis05]. The regions are illustrated in Figure 2.12.
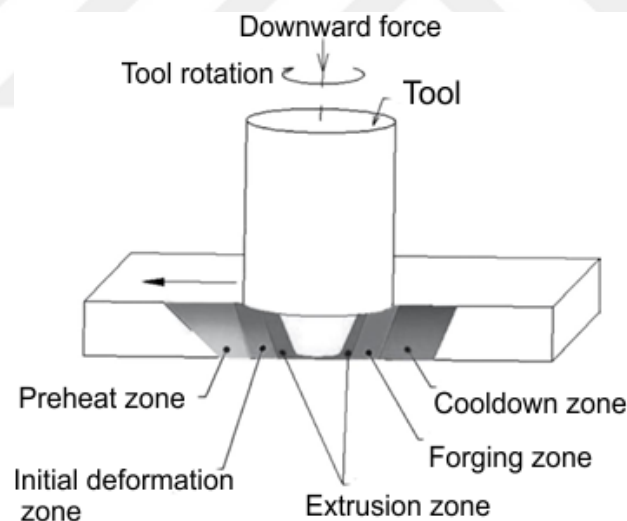
Figure 2.12: Welding zones according to Arbegast classification [Kha17]

In preheating zone in front of the tool pin, temperature increases because of the frictional heat from the rotating tool and adiabatic heat from material deformation; in this zone material does not undergo plastic deformation and the source of the heat results from the thermal field around the rotating tool. In the initial deformation zone, plastic deformation starts, and the shear stress is present in this region. Softened metal flow around the tool pin and is extruded from the front side to the backside of the tool in the extrusion zone. Forging zone is the region where material flowing around the pin of the tool is consolidated at the back of the tool pin by the forging effect from the tool. Tool shoulder facilitates the material constraint in

the cavity left by the advancing pin under hydrostatic pressure conditions and also realizes the forging effect by applied downward force. The following and the last region is a cool-down zone where the metal cools down, and the joint is completed [Kha17], [Mis05].
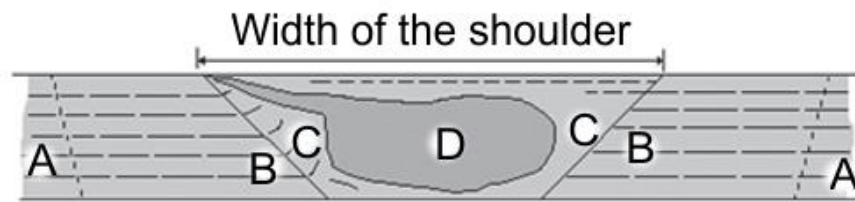
Figure 2.13: Welding zones according to Threadgill classification [Kha17] [Mis07] [Kum15]

Threadgill [Thr97] classified the welding zone into four zones based on the microstructure of the weld, as illustrated in Figure 2.13, as cited by Khan& Khan [Kha17]:

The stir zone (SZ), D region in Figure: In this zone, the tool pin stirs the material; SZ size is slightly wider than the diameter of the pin. Grain refinement occurs in SZ by severe plastic deformation and dynamic recrystallization [Thr97]. Heat resulting from friction and intensive plastic deformation creates recrystallized fine grains in the microstructure of the stir zone [Mis05]. Equiaxed grains have a remarkably smaller size in comparison with a base metal (BM). Onion ring shape can be observed in this region depending on the BM and the condition of the process, for the heat-treatable alloys, SZ has generally lower hardness value as compared to BM [Thr97].

The TMAZ, C region in Figure: TMAZ, thermomechanically affected zone, is an entirely deformed zone besides SZ, observable changes in microstructure occur as a result of deformation and thermal cycles experienced. Partial recrystallization in grains is seen with the effect of both lower temperature and deformation degree in comparison with SZ [Kha17]. However, Mishra and Ma [Mis05] stated that recrystallization did not occur in TMAZ because of inadequate deformation strain; even though, it experienced plastic deformation. Moreover, Mishra and Mahoney [Mis07] stated that the deformation is not sufficient to promote full recrystallization in spite of experienced deformation and heat. Locally high temperatures in TMAZ result in grain growth and partial dissolution of the precipitates, which then causes hardness value to reach a minimum in this region [Thr97], [Ole06].

The HAZ (heat-affected zone), B region in Figure: This is a common region for all welding techniques. Even though there is no deformation in this zone; it is influenced by the heat. The microstructure in HAZ resembles the BM. Hardness usually drops in HAZ for the welding of heat-treatable aluminum alloys showing the effect of the thermal cycle [Kha17].

The BM, base material or unaffected material, A region in Figure: Although thermal cycle may exist in this zone, it does not cause significant microstructure changes [Kha17].

FSW obtains fine recrystallized equiaxed grains in the stir zone as a result of both intense stirring and high temperatures; the bending of the grains is detected in the TMAZ as a consequence of plastic deformation [Sha16]. It is also noted that larger shoulder diameters result in wider TMAZ through expanded contact area. [Sha16].

2.3.3 Tooling of FSW

The FSW tool has three main tasks: Firstly, it heats the workpiece; secondly, it moves the material in order to achieve joining; lastly, it contains the hot metal below the tool shoulder [Kum15]. The tool and its parameters are illustrated in Figure 2.14.
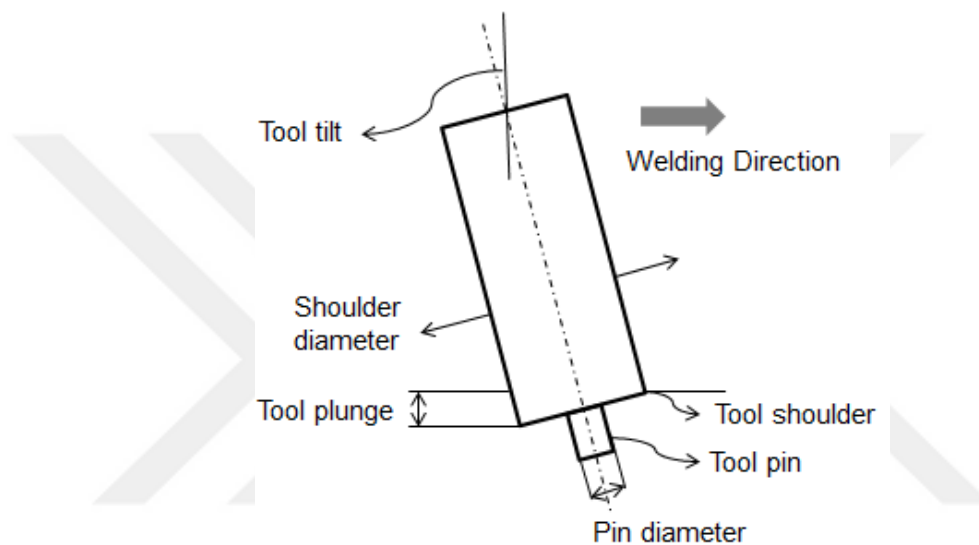
Figure 2.14: FSW tool and tool-related welding parameters

The biggest part of heating results from the friction between the workpiece and the tool shoulder. In terms of heating, the most critical design aspect is the pin/shoulder relative size; other design aspects are relatively less crucial. Moreover, another tool function is to stir and put the material in motion. Tool design governs the microstructure uniformity and its properties, also process loads [Mis05].

High temperature, abrasive wear, and dynamical impacts have significant effects on the tool during the process. Consequently, the desired material properties for the tool are listed as: Sufficient toughness; sufficient strength at high temperatures and temper resistance; good wear resistance [Mei13]. It can be said that tool geometry, as well as tool material, are two crucial parts of tool design in FSW. The material properties needed to be considered is as follows: Wear resistance; reactivity of the tool; thermal expansion coefficient; fracture toughness; stability at elevated temperature; good strength both at ambient and elevated temperatures; and machinability [Mei13]. Moreover, tool material has an effect on the reached temperature at the stir zone of the weld; the thermal conductivity of workpiece and tool material and the friction coefficient between workpiece and tool decide sufficient heat

generation and distribution at tool and workpiece interface [Kha17]. Another important property for tool material in case of numerous cycles of heating and cooling is thermal fatigue strength [Mis07].

The tool shoulder confines the material from expelling and exerts forging force for consolidation of the metal behind the tool pin [Kum15]. There are several shoulder designs, and each of them provides different benefits. For instance, the concave tool is one of the most common shoulder design preferred since, in concave tool, the softened material is stored inner side of the concave region just as a reservoir and minimize the formation of flash and provides sound welds [Ull17], [Kha17]. Furthermore, the scrolled shoulder is not recommended to use for the welding of the different thickness plates; otherwise, flash formation will occur from the thicker workpiece [Mis07]. Several tool shoulder designs are illustrated in Figure 2.15.
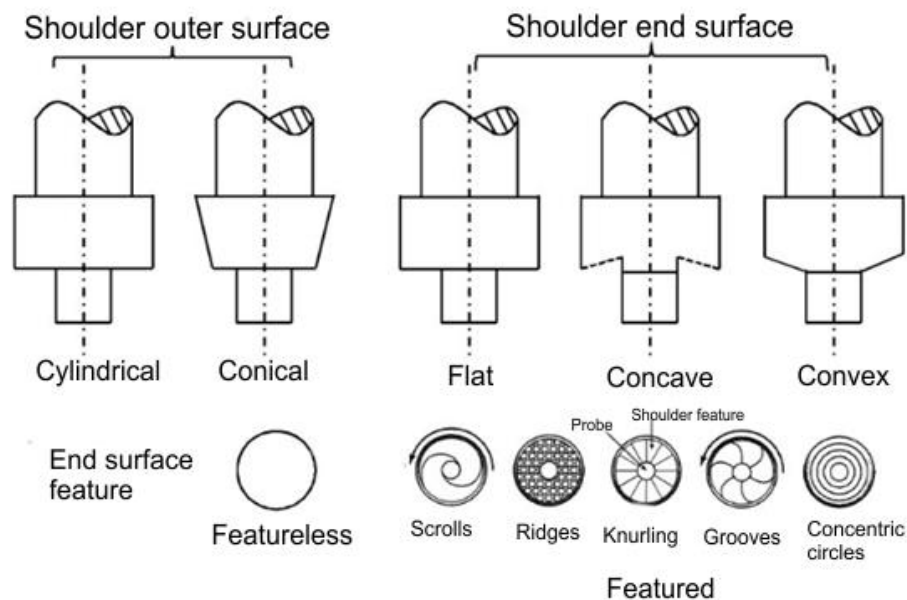

Figure 2.15: Tool shoulder designs [Zha12]

Tool pin disrupts the contact surfaces of the plates to be welded, shear the material on ahead of the tool, and transfer the material back of the tool; it also governs the deformation depth [Mis07]. Even though the properties of the weld, the loads on the tool, and weld defects are influenced by the tool design, the cross-sectional geometry of the pin and surface details on the pin such as threads affect the rates of heat generation, the flow of material, and axial forces [Cha15]. Zhao et al. [Zha05] investigated the effect of pin geometry on friction stir weld 2014 alloy, and they concluded that when there is no screw thread on the pin, the interface of TMAZ and stir zone is very obvious because of poor material flow and higher rates of speed. Also void defects were observed in case of welds performed with unthreaded pins [Zha05]. Pin profiles are summarized in Figure 2.16.
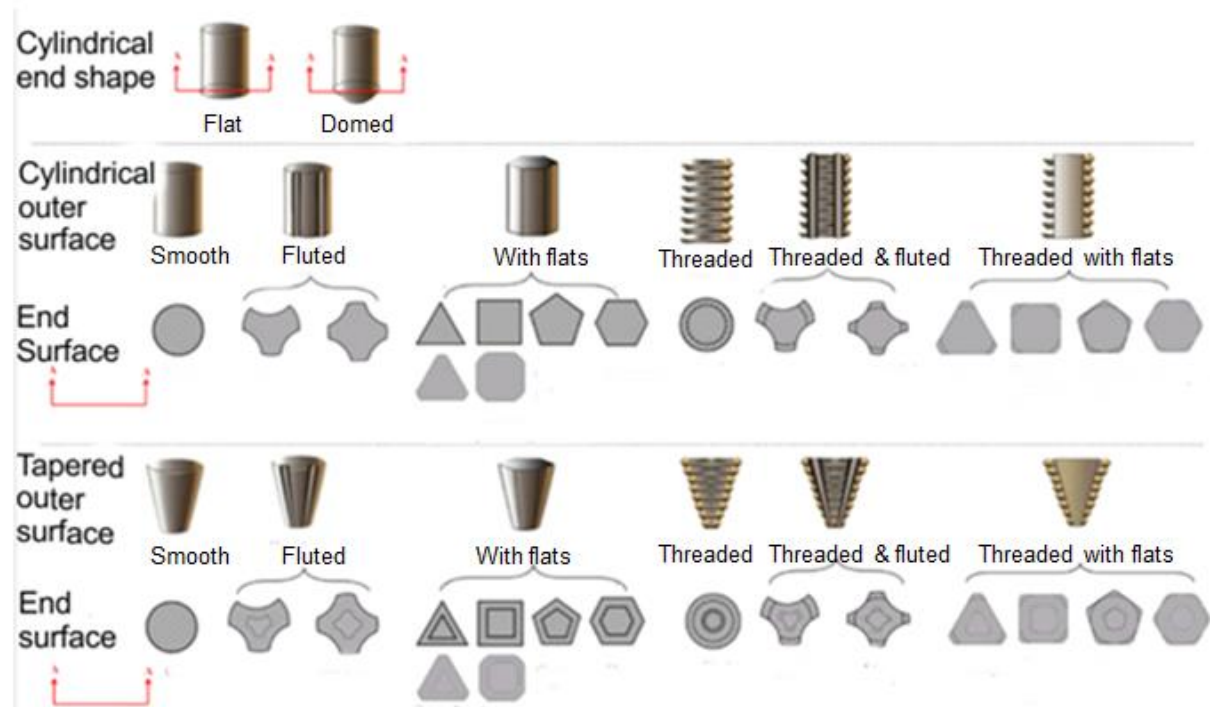
Figure 2.16: Tool pin designs [Zha12]

Tools can be divided into three categories, as shown in Figure 2.17: Fixed, adjustable and bobbin type tools. Whereas adjustable pin provides adjustment of the length, thusly, elimination of exit hole at the end of the weld, bobbin tools eliminates incomplete root penetration and enables higher welding speeds because of heat arising from two shoulders [Mis07].
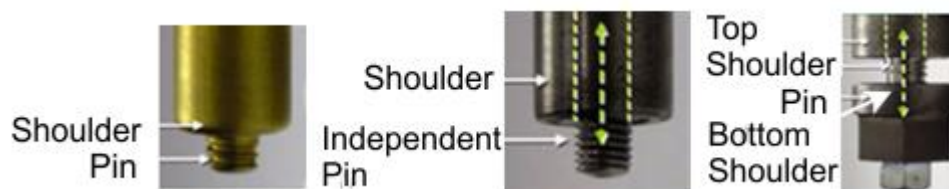
Figure 2.17: Types of tools [Mis07]

2.3.4 Process Parameters for FSW

Several factors have effects on the friction stir welding process, the incoming factors including tool design, machine, etc. and the outputs from the process such as microstructure, mechanical properties are listed in Figure 2.18.
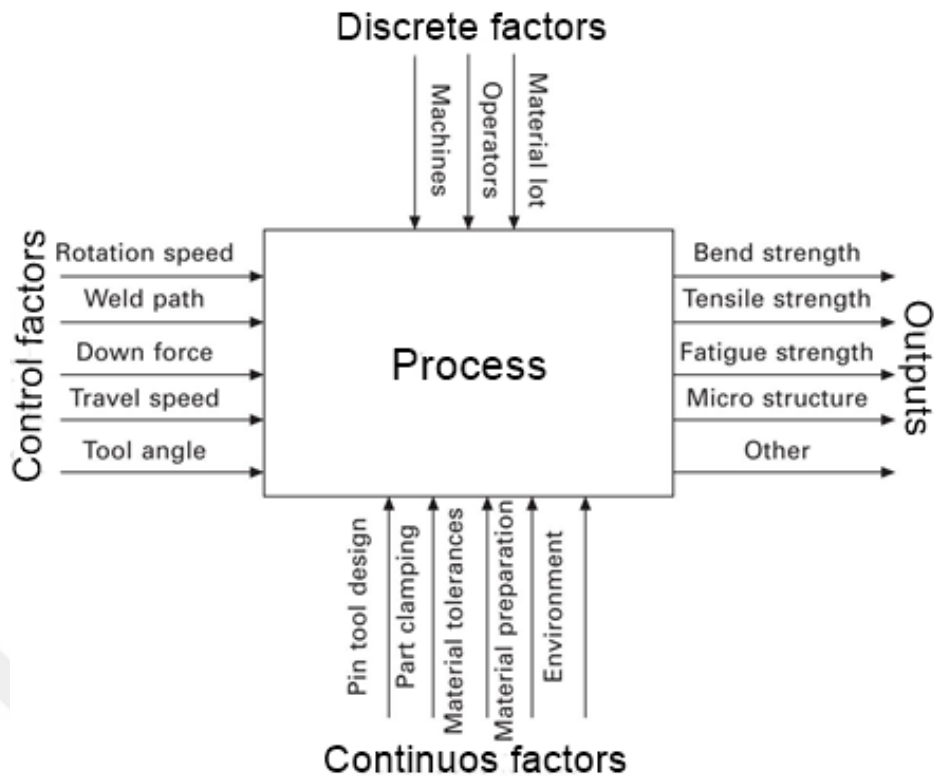
Figure 2.18: DOE FSW process schematic [Loh10]

Two process parameters for FSW are crucial among others: Tool rotational speed (rpm) and tool traverse speed (mm/min), also named as welding speed, which is also the main focus of this study. Tool rotation providing stir and mix action, together with tool traverse transferring the stirred metal front to the back of tool pin have a great impact on temperature development. Higher rotational rates produce higher temperatures as a result of increased frictional heat and lead to more intensive stir and mix action [Mis05]. As cited by Lohwasser and Chen [Loh10] several studies [Yan07], [Col07], [Pee06] have indicated that the effect of tool rotation rate considerably greater effect on mechanical properties and microstructure than the welding speed and axial load. Plunge depth is another vital parameter for heat generation and the forging action in FSW. High plunge depth generates higher heat generation, hereby larger grain size and IMCs formation affecting joint ductility and strength whereas low plunge depth leads in inadequate plasticization and mixing of the material, which triggers the formation of weld defects, as a result of lower heat input [Kha17].

There are many other parameters affecting the quality of the weld; however, it is generally not very simple to establish robust understanding on the input/output factors' relationships for FSW process due to both thermomechanical characteristics of FSW and remarkably complex flow of material in FSW [Kum15].

2.3.5   Effects of Process Parameters on Weld Properties

Kasman, Kahraman, and Aydin [Kas16] have investigated mechanical properties of the friction stir butt-welded AA7075-T651 plates with using three different tool pin designs (triangular, pentagonal, helical) at two different rotational speed and concluded that for the same pin profiles, tensile strength is increased with increasing rotational speed. Cevik, Ozcatalbas, and Uygur [Cev12] have studied 7075-T651 Al-alloys joined by FSW at three different welding speeds and investigated hardness and microstructure of the specimens, and concluded that hardness increases with increasing welding speed.

Cavaliere, Squillace and Panella [Cav08] have investigated the welding speed effect (40–460 mm/min) on microstructure, and mechanical properties of friction stir welded AA6082 alloy. They showed that the increase in the welding speed results in uniform and fine grain distribution in SZ; in addition, strength increases with increasing welding speed up to 115 mm/min, beyond it dropped. As cited by Mishra and Ma [Mis05], Biallas et al. [Bia99] examined the parameters for FSW process of 2024Al-T4 and concluded that yield and tensile strengths increase with increasing tool rate for a constant tool traverse speed/rotation rate ratio; also ductility is improved. As cited by Khan and Khan [Kha17], Li and Liu [Li13] has investigated the effects of welding speed on mechanical properties and microstructures of AA2219-T6 welded by the reverse dual-rotation friction stir welding. They found out that microhardness of TMAZ and HAZ increases gradually with increasing weld speed, from 50 to 200 mm/min, as a result of restrictions in the dissolution of the precipitates and grain growth; moreover, tensile strength raised as the welding speed increased up to 150 mm/min, then decreased, the reason of the lower tensile strength at low welding speed is that higher holding time and heat input results in growth of the grains. Golezani et al. [Gol15] studied the effect of tool rotational speed in friction stir welding of 7020-T6 aluminum alloy, and revealed that SZ has finer grains than BM, the size of the grains in SZ increased with increasing rotation rate, which also causes the microhardness to drop. They concluded that larger grain size and subsequently lower microhardness are caused by too high heat input at higher rotational speed. Moreover, Khan and Khan [Kha17] stated that precipitates coarsen and dissolve at higher rotation speeds as a result of greater heat generation whereas, at lower rotational speed, insufficient heat input result in improper mixing of material flow. Also, they indicated that increasing rotational speed leads to increase in tensile strength up to a point, and then it decreases.

2.3.6   Welding Defects

FSW, as a solid phase process, does not include bulk melting of the base metal at the weld joint; therefore, problems encountered in fusion welding processes such as hot cracking and

porosity are eliminated in FSW. Reasons for defect formation are more related to imbalances in the flow of the material or geometrical issues in association with tool position relative to the joint [Loh10].

Main parameters for heat input is tool rotation, and welding speed, as illustrated in Figure 2.19 defects may arise outside the marked region. The outside regions can be introduced as following flaws: (1) Excessive flash arising from high heat input; (2) Groove-like or cavity flaw due to the inadequate heat input; (3) Cavity generated by the abnormal stirring [Pod15].
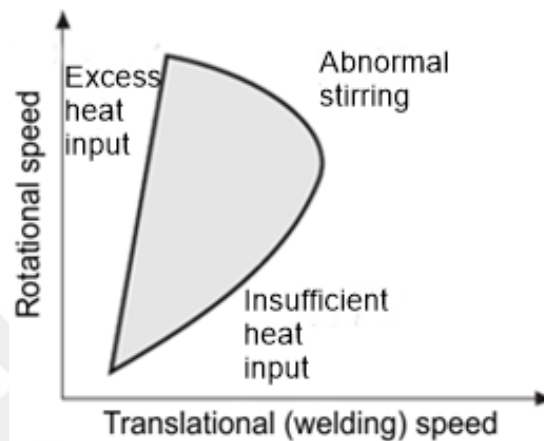
Figure 2.19: Mutual effects of rotational speed and welding speed [Pod15]

In FSW, flaws such as formation of voids, kissing bond (KB), nonbonding, tunneling defect, hooking defect and joint-line remnant (JLR) can arise in case of very cold weld state, as a result of poor material flow (lack of softening and insufficient mixing) whereas defects like formation of flash, nugget collapsing at the stir zone can develop in case of very hot weld state, as a result of excessive flow of material [Kah15], [Kha17]. Moreover, the formation of intermetallic compounds (IMCs), which are brittle and hard causing deterioration in weld strength, can occur in higher heat input case; consequently, optimal heat input has a crucial impact on the defect-free weld formation [Kha17].
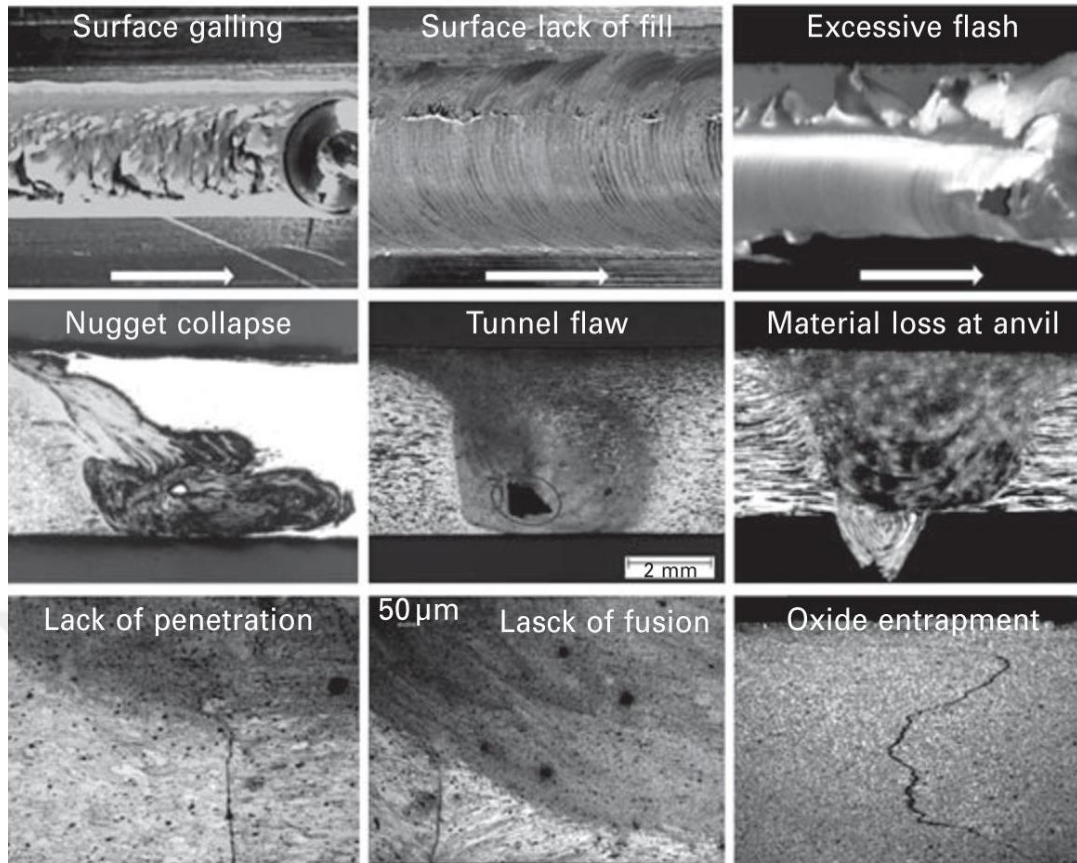
Figure 2.20: Characteristic flaw types in friction stir welds [Loh10]

Furthermore, geometry-based defects such as lack of penetration can be seen as a result of incorrect tool design or operator errors [Kah15]. Some of the common defects in FSW is illustrated in Figure 2.20.

2.3.7 FSW of Dissimilar Alloys

During FSW of dissimilar alloys, in addition to the parameters of FSW of similar alloys, some more crucial process parameters are included in the process; these parameters are tool pin offset, position of the plates to be welded. Tool pin offset, tool axis shift on one of the sides of the joint, is decided so that tool stirs comparably more volume of weaker metal, which is also softer, in order to achieve sufficient blend of two metal during stirring. Moreover, balance in flow stress, which provides elimination of tunnel effect and improved joint strength, is accomplished by the balance of the heat between stronger and weaker metals during movement of metals. When pin offset is set to zero for dissimilar welding, it will lead to equal heat generation causing non-uniform softening and imbalanced flow stress [Kha17].

As cited by Abd El-Hafez and El-Megharbel [Abd18], Xue et al. [Xue11] and Jata et al. [Jat01] affirmed that when hard metal is located at AS, joint strength will be enhanced, whereas Khodir and Shibayanagi [Kho08] asserted that in order to improve weld quality, plate with

lower strength should be located on AS. Consequently, opinions on the position of the plates for improved weld quality remain contradictory.

Plunge depth is another important parameter for dissimilar welding process of FSW. In case of low depth of plunge, insufficient material flow as a result of low forging action and poor bonding between dissimilar parent metals leads to tunneling defect and KB defect, which deteriorates joint strength. The opposite case, excessive depth of plunge, causes the excessive formation of flash, thinning of the joint, and overheating. Moreover, overheating leads to the intermetallic compound formation and strengthening precipitate dissolution and coarsening of the grains, which affect the joint strength adversely [Kha17]. For successful processing, the optimum solution is required.

Furthermore, welding speed and rotational speed of the tool will also affect the degree of the intermixing of two dissimilar materials [Kum15].

2.3.8 Advantages and Disadvantages of FSW

As all joining processes, FSW has both advantages and disadvantages. Mishra and Ma [Mis05] summarized the key benefits of the process as in Table 2.3. Namely, the advantages are divided into three categories: Metallurgical, environmental and energy. The discussion between fusion welding and FSW has been introduced in the previous chapters in detail.

Table 2.3: Metallurgical, environmental and energy benefits of FSW [Mis05]

Metallurgical benefits	Environmental benefits	Energy benefits
Solid-phase process	No shielding gas required	Improved materials use (e.g., joining different thickness) allows a reduction in weight
Low distortion	Minimal surface cleaning required	Only 2.5% of the energy needed for a laser weld
Good dimensional stability and repeatability	Eliminate grinding wastes	Decreased fuel consumption in lightweight aircraft, automotive, and ship applications
No loss of alloying elements	Eliminate solvents required for degreasing	
Excellent mechanical properties in the joint area	Consumable materials saving, such as rugs, wire, or any other gases	
Fine microstructure		
Absence of cracking		
Replace multiple parts joined by fasteners		

The limitation of the process is listed as follows by Paik [Pai09]:

- Tool pins in FSW are consumable; also, the size of the pin is dependent on the workpieces to be welded.
- FSW machine is not capable of all of the welding positions such as fillet weld due to its limited orientation. However, butt and lap joints are accomplished with the FSW process.
- Formation of keyholes occurs at the end of the weld.
- When compared to fusion welding, FSW is performed at slower rates.

Another important drawback of the process is that FSW requires high capital investment; however, modification of the heavy-duty vertical milling machines makes the process performable [Kha17].

3 Experimental Methods

3.1 Experimental Setup

3.1.1 CNC Machine Used in FSW Process

Friction stir welding process is performed at the 5-axis CNC machine, Mazak VTC-800/30SR. The capacity of the machine is given in Table 3.1.

Table 3.1: Capacity of Mazak VTC-800/30SR

Property	Unit	Maximum Value
Spindle Speed	min-¹	18000
Feed rate	m/min	50

3.1.2 Workpiece Properties

In this study, two different plates are used: AA 6082 and AA 6005 series aluminum alloys, the size of each plate to be welded are 200x90x3.9 mm; the plates are products of extrusion process and prepared to the specified size in order to conduct FSW trials on CNC machine.

The chemical composition of the aluminum alloys is stated in Table 3.2.

Table 3.2: Alloying elements for AA 6005-T6 and AA 6082-T6

Aluminum Alloy	Alloying Element (%)							
	Si	Fe	Cu	Mn	Mg	Cr	Zn	Ti
6005-T6	0.6-0.9	0.35	0.1	0.1	0.4-0.6	0.1	0.1	0.1
6082-T6	0.7-1.3	0.5	0.1	0.4-1	0.6-1.2	0.25	0.5	0.1

Some of the properties of aluminum alloys are listed in Tables 3.3 and 3.4.

Table 3.3: Some physical and thermal properties of AA 6005-T6 and AA 6082-T6

Aluminum alloys	Thermal conductivity	Density	Specific heat	Thermal expansion coefficient
	W/m.K	g/cm³	j/Kg.K	µm/m.K
6005-T6	193	2.71	892	23.3
6082-T6	216	2.7	894	23.1

Table 3.4: Mechanical properties of AA 6005-T6 and AA 6082-T6

Aluminum alloys	Tensile strength	Yield strength	Elongation	Hardness
	MPa	MPa	%	HBW
6005-T6	270	225	8	90
6082-T6	290	250	8	95

3.1.3 Fixture Design

The fixture is one of the crucial components of a successful FSW process. Baghel and Siddiquee [Bag12] have stated that there are several key considerations when designing a fixture for FSW process. First of all, in FSW, tool is subjected to axial forces with an amount depending on several factors including the tool, workpiece material, and thickness, welding speed, etc. This force must be in control in order to prevent deflection. Secondly, during plunge step, lateral loads arise and cause separation of the workpieces along the joint line; besides, thermal expansion/shrinkage on plates as tool passes increases the tendency to the

separation, as a result of an in-plane moment. Therefore, lateral restraining of the plates and clamping at the plate end are significant for successful joining. However, this restraining may lead to the upward buckling of the plates, as a counteraction, the clamping should ensure application of out-of-plane loads, hindering buckling. Another point is prevention of the sliding of the plates longitudinally, which is especially critical for corner joints [Bag12].
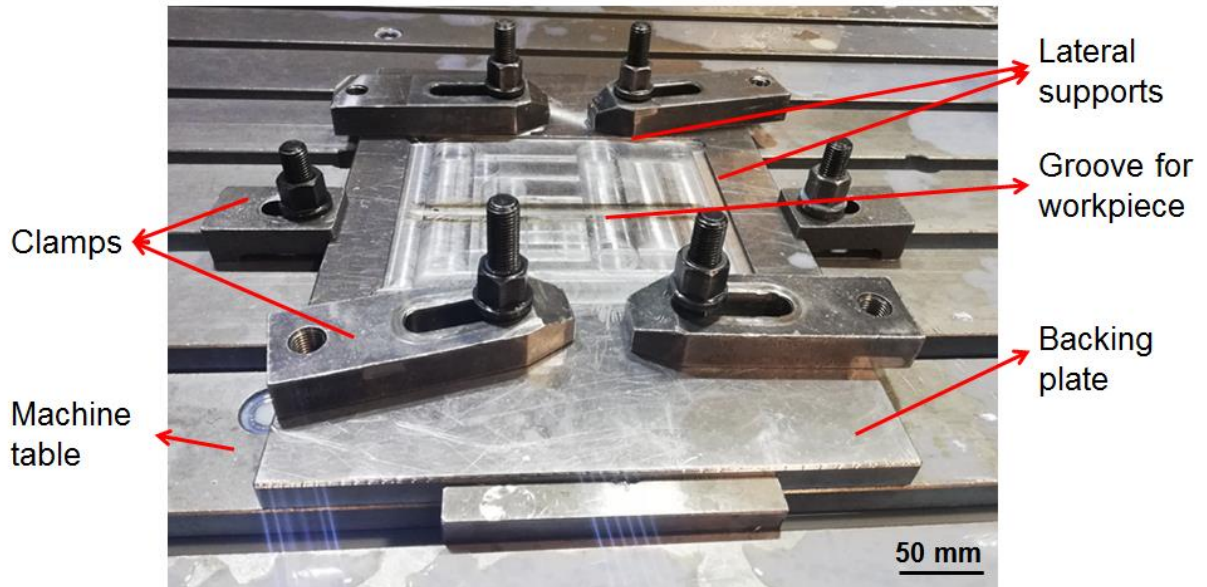
Figure 3.1: Fixture and its components

The fixture used for this study is shown in Figure 3.1. AISI-1050 carbon steel is used for the fixture of the friction stir welding. Several cautions are taken for keeping the position of the workpieces fixed and secure in order to obtain successful welding processes. For both fixing and supporting purposes; additionally, groove in the dimensions of the aluminum plates to be welded were machined onto backing plate. By that way, the adverse effects of the lateral forces and possible deflections are aimed to be eliminated. Moreover, clamps were used not only for fastening the backing plate on the machine table of the milling machine, but also for the fixing the workpiece onto backing plate. During the processing, it was observed that the fixture provided secure clamping of the workpiece.

3.1.4 Tool Design

Tool design has a great effect on the process quality in friction stir welding. Emamian et al. have reported that researches done recently on FSW showed that pin profile has very crucial effect on the flow of material and mechanical properties, also he observed that square pin profile, threaded cylinder or threaded taper pins provide sound joints, and in almost all studies, threaded pins gave the most effective results in terms of tool performance [Ema17].

In addition, Zhao et al. have concluded that threaded pins are better since they improve the flow of the material by implying downward force on material. Also more heat input will be

obtained as a result of higher heat generation compared to thread-free pins [Zha05]. Moreover, they concluded that among column screw, column pin, taper pin, and tapered screw tool pins, tapered screw tool pin resulted in 75% of the tensile strength of the base material. Venkateswarlu et al. have emphasized that apart from threaded pin profiles, concavity of the shoulder is another significant dimension of the tool. Furthermore, Aissani et al. have reported that a cylindrical threaded pin with a concave shoulder has been used by the majority of the researchers [Ai10]. Ullegaddi et al. stated that concave shoulder generates sufficient temperature to obtain good weld meanwhile ensuring that the temperature stays below the melting temperature of the base metal as a result of high normal force as compared with other tools, i.e. it softens the metal and forms good joint in comparison with other different tool shoulders [Ull17].

The dimension of the pin is another important parameter in tool design. Ullegaddi et al. reported that the pin length is generally slightly less than the workpiece thickness, and its diameter is usually slightly larger than the workpiece thickness [Ull17]. Mohanty et al. stated that the pin diameter is equal to workpiece thickness, and the pin length is slightly shorter than the workpiece thickness [Moh12]. It has been observed from the previous studies on tool design for FSW that the diameter ratio between a pin and a shoulder is usually kept around three. In Figure 3.2, dimensions and manufactured form of the tool are given.
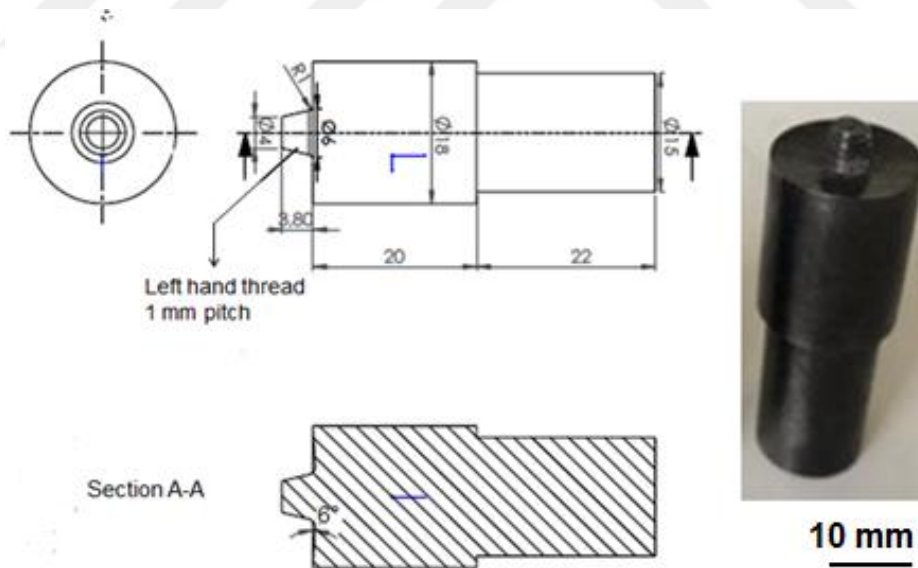
Figure 3.2: Manufactured Tool 3 and technical drawing of Tool 3

In this study, two different tool pin design were used: Cylindrical threaded pin and a tapered threaded pin. The main trials were performed with tapered threaded pin with concave shoulder. The pin length is designed as 0.2 to 0.3 mm shorter than the thickness of the workpiece.

The tool material was selected as AISI-H13 steel, which was heat-treated to improve its hardness to approximately 55 HRC. AISI-H13 has good resistance to thermal shock, high toughness and good wear resistance at high temperatures; moreover, thanks to its good thermal conductivity, the heat resulted from welding process will be easily removed from the tool [Mal10]. AISI-H13 is mainly used in extrusion dies for aluminum alloys, injection molding dies for metallic parts, and hot forging dies, etc. The alloying elements of the material are given in Table 3.5. [NN13].

Table 3.5: Alloying elements for AISI-H13 steel

Alloying Element (%)

C	Si	Mn	P	S	Cr	Mo	V	W	Ni
0.32-0.45	0.80-1.20	0.25-0.50	0.025	0.002	4.75-5.50	1.10-1.75	0.80-1.20	-	-

3.2 Initial Trials

3.2.1 Trials with 3-axis Milling Machine

Figure 3.3: 3-Axis milling machine

The first trials were conducted at the conventional 3-axis milling machine, as shown in Figure 3.3, with tool 1, which is shown in Figure 3.4. The material for tool 1 is AISI-1045 steel without subsequent heat treatment; the alloying elements of the material are given in Table 3.6.
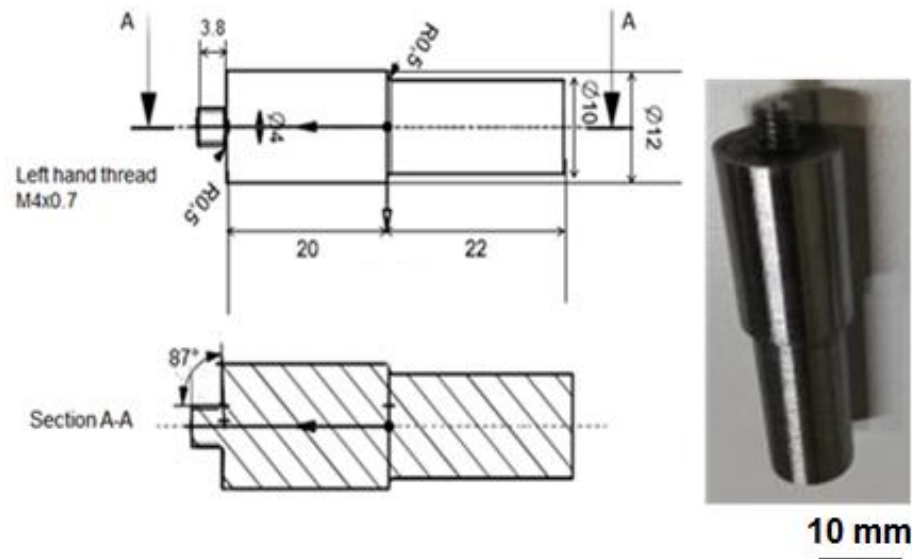
Figure 3.4: Manufactured Tool 1 and technical drawing of Tool 1

Tool 1 was designed after the review of the previous studies. The ratio between shoulder diameter and pin diameter were three, and the diameter of the pin is almost equal to the thickness of the parts to be welded.

Table 3.6: Alloying elements for AISI-1045

<div align="center">

Alloying Element (%)

</div>

C	Si_{max}	Mn	P_{max}	S_{max}	Cr	Mo	V	Ni
0.32-0.50	0.40	0.50-0.80	0.035	0.035	-	-	-	-

At first trials, after the dwell period, just as the tool started advancing motion along the weld line, the tool has broken at the root of the pin, as stated in Figure. It is presumed that tool 1 could not resist highly dynamical impacts resulting from the nature of the FSW. It is also observed that the material for FSW tool should have sufficient toughness and strength with improved hardness properties which will require subsequent heat treatment after machining of the tool to the desired geometry.
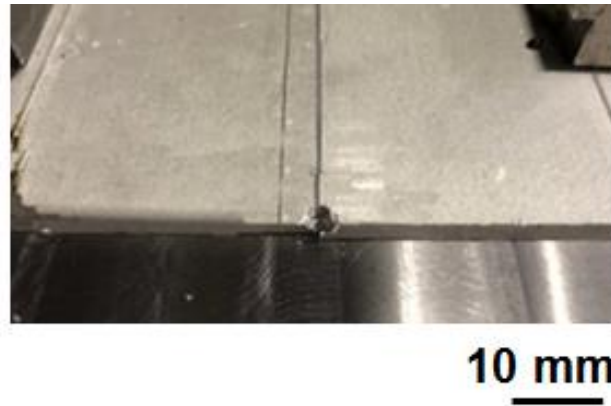
Figure 3.5: Tool breakage of tool 1

After the breaking of the tool 1, the design is modified to the tapered threaded tool pin, as shown in Figure 3.5. Modifications such as increasing the pin and the shoulder diameter and increasing the radius between tool pin and tool shoulder in order to overcome stress concentration causing failure of the tool. The material of the tool was changed to AISI-H13 hot work tool steel, and the tool was heat-treated to obtain hardness approximately at 55 HRC. AISI-H13 has high strength at high temperature, high toughness, good thermal fatigue resistance, and good machinability [NN19].
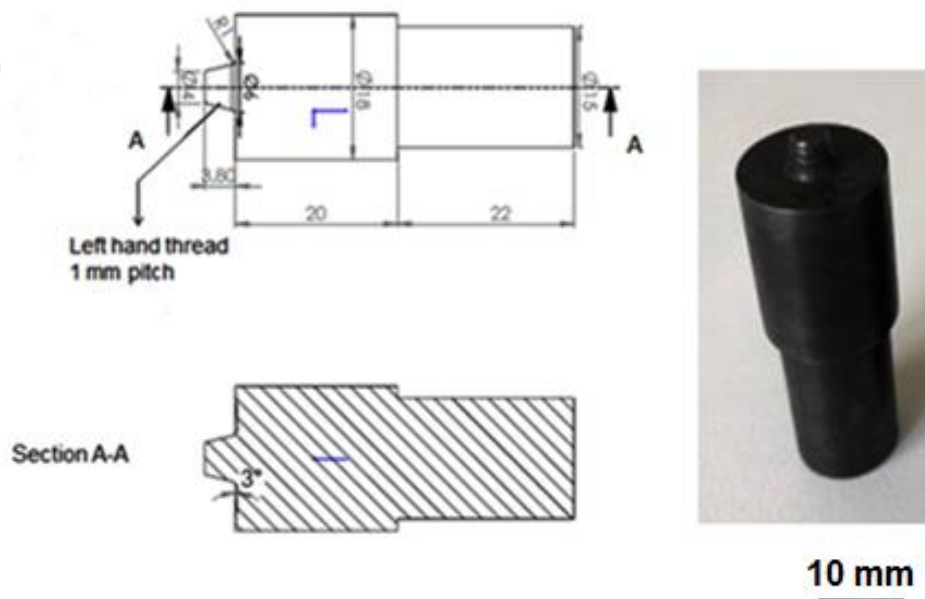
Figure 3.6: Manufactured Tool 2 and technical drawing of Tool 2

Initial experimental trials were performed with tool 2 with MazakVTC-200C-II 3-axis CNC machine; some samples from the trials are shown in Figure 3.7. Since the trials were carried out at 3-axis CNC machine, the tool could not be tilted by some degree in order to provide tilt angle. As can be seen from Figure 3.7, excessive flash formation occurred during most of the parameter sets including various rotational speed and welding speeds.

Figure 3.7: Excess flash formation

3.2.2 Trials with 5-axis CNC Machine

The effect of the tilt angle is emphasized many times in the previous studies on FSW; moreover, researchers noted that the proper usage of the concave tool shoulder requires a tilted tool in the welding process. Tilt angle provides better recoalescence of the material at the back of the tool in the nugget zone [Sha16].

Figure 3.8: Defective joints

For the trials with 5-axis CNC machine, the tool was also improved to tool 3, which is shown in Figure, the concavity of the shoulder was increased from 3 º to 6 º as a prevention of the excess flash formation. However, in the first trials, excessive flash formation with hot tearing was observed as shown in Figure 3.8. This problem is reported to be related with hot weld conditions; nonetheless, the problem continued at trials which are done at colder conditions; in other words, at lower rotational speed and/or higher welding speed. Therefore, other solutions were tried to be found for the problem and it was found that when the rotation orientation of the tool was changed from clockwise rotation to counterclockwise rotation, the formation of flash disappeared; even though, some researchers claimed that the proper usage of the left hand threaded pin is managed with clockwise rotation of the pin. The mechanism of this solution can be explained as in Figure 3.9. Panneerselvam and Lenin studied on the joining of Nylon 6 plates by friction stir welding with main focus on orientation of a tool rotation with left hand threaded profiled pin design. They concluded that counterclockwise rotation resulted flawless welds with better weld properties [Pan14]. They also illustrated the movement of the material in both orientations, as it can be seen from

figure 3.9(a), in clockwise direction, the material was thrown out through the flute of the thread.
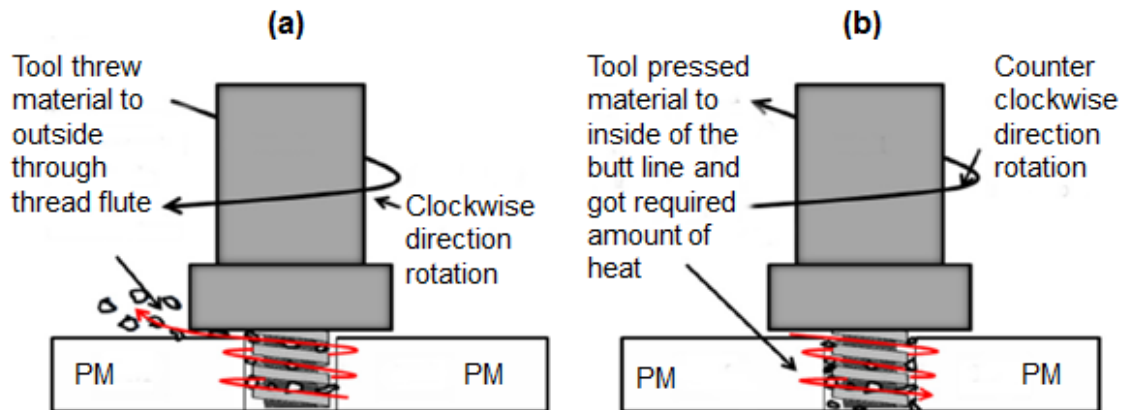
Figure 3.9: The effect of the tool rotation in clockwise (a) and counterclockwise (b) [Pan14]

Nevertheless, Nylon 6 and aluminum alloys have quite different material properties, the movement of the material during the welding process are similar, the flash formation, mainly on RS of the weld, also supports the illustration in Figure. Furthermore, Barlas and Ozsarac [Bar12] have investigated the effects of FSW parameters on weld properties of AA 5754 aluminum alloys and found out that sound welds were obtained in the counterclockwise tool rotation. Therefore, tool was decided to be rotated in counterclockwise direction throughout experiments.

The workpieces (plates) were cleaned prior to welding process with the help of acetone and steel wire brush in order to remove dirt, and any left particles from machining process.

3.3 Test Plan

The detailed test plan for this study is given in Table 3.7.

Table 3.7: Test Plan

No	Tool Rotation Speed	Welding Speed	Advancing Side (AS)	Retreating Side (RS)	Tilt Angle
	rpm	mm/min	-	-	°
1	1200	70	6082	6005	2
2	1200	110	6082	6005	2
3	1200	150	6082	6005	2
4	1500	70	6082	6005	2
5	1500	110	6082	6005	2
6	1500	150	6082	6005	2
7	1800	70	6082	6005	2
8	1800	110	6082	6005	2
9	1800	150	6082	6005	2
10	1500	70	6005	6005	2
11	1500	110	6005	6005	2
12	1500	150	6005	6005	2
13	1800	150	6005	6005	2
14	1500	70	6082	6082	2
15	1500	110	6082	6082	2
16	1500	150	6082	6082	2
17	1800	150	6082	6082	2
18	1500	150	6082	6005	3
19	1500	150	6005	6082	2

In total, four different sets of experiments were carried out as shown in Table: The first set, from 1 to 9 is dissimilar welding of 6082 to 6005, and the second set, from 10 to 13, is similar welding of 6005 to 6082, the third set, from 14 to 17, is similar welding of 6082 to 6082, and

the last set including 18 and 19 was carried out in order to understand the effect of tilt angle and the position of the welding plates in dissimilar welding of 6005 and 6082.

The tool plunge depth was 0.5 mm and the dwell period was kept at 15 seconds for each experiment. The tool was rotated in counterclockwise orientation.

The position of the plates at welding is a controversial issue among the researches. Khodir and Shibayanagi [Kho08] obtained higher tensile strength in the longitudinal direction when the stronger material placed at AS; however, joint showed higher tensile strength in transverse direction when softer material placed in AS. Kumar et al. stated that material with higher melting point is often fixed on AS in butt joint welding; also tool offset is provided from butt interface toward the material with lower melting point to avoid overheating in material with lower melting point and tool wear [Kum15]. For welding of aluminum with steel when steel being harder material is placed on AS successful joint obtained since when the material on RS stays too rigid during welding, the material transportation around the tool pin will be restricted [Loh10].

In this study, even though the material properties of the two materials are not very different, the relatively harder material, AA 6082, was placed on AS during the most of the specimen sets except for specimen 19.

4 Results

For this study, as explained in the test plan, friction stir welding was carried out for nineteen specimens, the main aim of the study was to find the optimal welding parameters for the friction stir welding of the 6000 series aluminum alloys; for this reason, the study has focused union the two of the most significant process parameters: Rotational speed and welding speed. Apart from those parameters, effect of the tilt angle and effect of the welding position for the dissimilar welding was investigated. For the determination of the weld quality, various tests were conducted. The tensile tests and microhardness tests were done for the investigation of the mechanical properties of the weld joints. The macrographs were taken in order to detect the visible flaws at the weld zone and to check the weld zone with the main lines. The microstructure of the weld was examined with both the optical microscope and the scanning electron microscope (SEM); in this way, the more accurate analysis and relations within the different testing methods were aimed to be obtained.

In Figure 4.1, the appearance of the weld seams for the dissimilar friction welding between 6082 and 6005 are shown. It can be observed that for all specimens there is no flash formation detected. It can also be seen that for the specimen 1, 2 and 3 at the exit hole of the weld, weld bead shows unsteady material flow, the reason can be that near the end point of weld bead at lower rotational speeds there is insufficient heat input, which results in inadequate flow of the material. This problem is apparently eliminated at the higher rotational speeds.
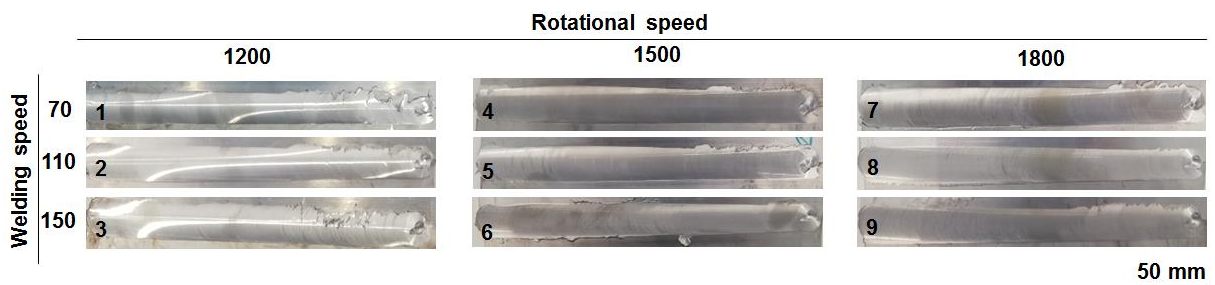
Figure 4.1: Appearance of the weld bead for dissimilar welding set from specimen 1 to 9

The weld beads from the similar welding of the 6005 and 6082 are separately illustrated in Figure 4.2.
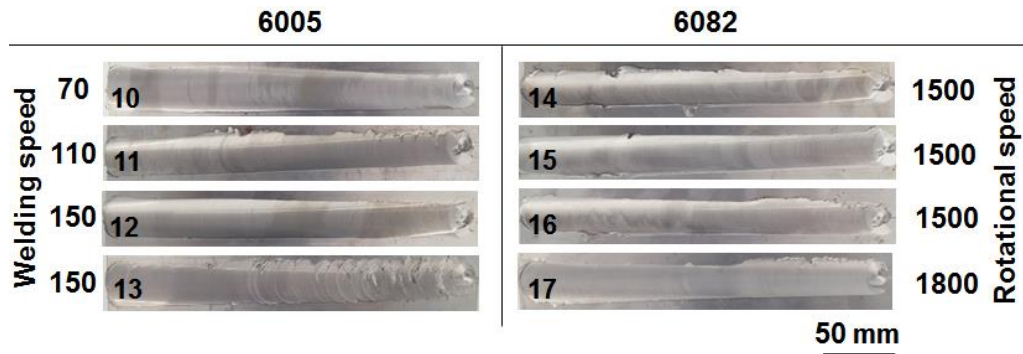
Figure 4.2: Appearance of the weld bead for similar welding set from specimen 10 to 17

Except for specimen 13, there are no flaws observed from the visual inspection of the weld beads. The turbulent flow of the material near the exit hole of the weld is observed at specimen 13. The reason can be the abnormal stirring as the rotational speed was increased at high welding speed.
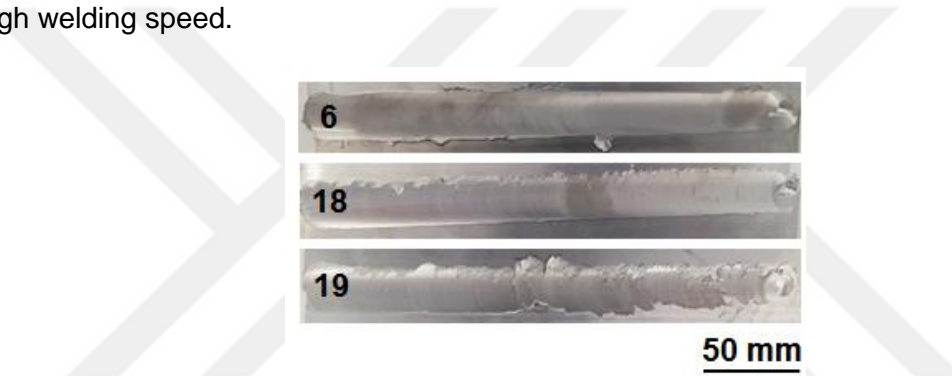
Figure 4.3: Appearance of the weld bead for the observation of the effect of tilt angle and weld position in dissimilar welding

In Figure 4.3, specimens of dissimilar welding process at constant rotational and welding speed are shown. Specimen 6 and 18 can be said to be flaw-free for the visual inspection; nonetheless, specimen 19, whose difference from the specimen 6 is the welding position of the dissimilar aluminum plates in the process, showed flash deformation mainly at the retreating side, and turbulent flow near the exit hole of the weld seam.

4.1 Tensile Test

Tensile tests were conducted with universal tensile testing machine Zwick/Roell Z050, whose maximum testing force is 50 KN. The specimen elongation was measured directly on the specimens by means of a tactile extensometer; the gauge length is 50 mm. Tensile tests were performed according to DIN EN ISO 6892-1 [DIN10] standards. The testing speed is 10 mm/min. The tensile test machine is shown in Figure 4.4.
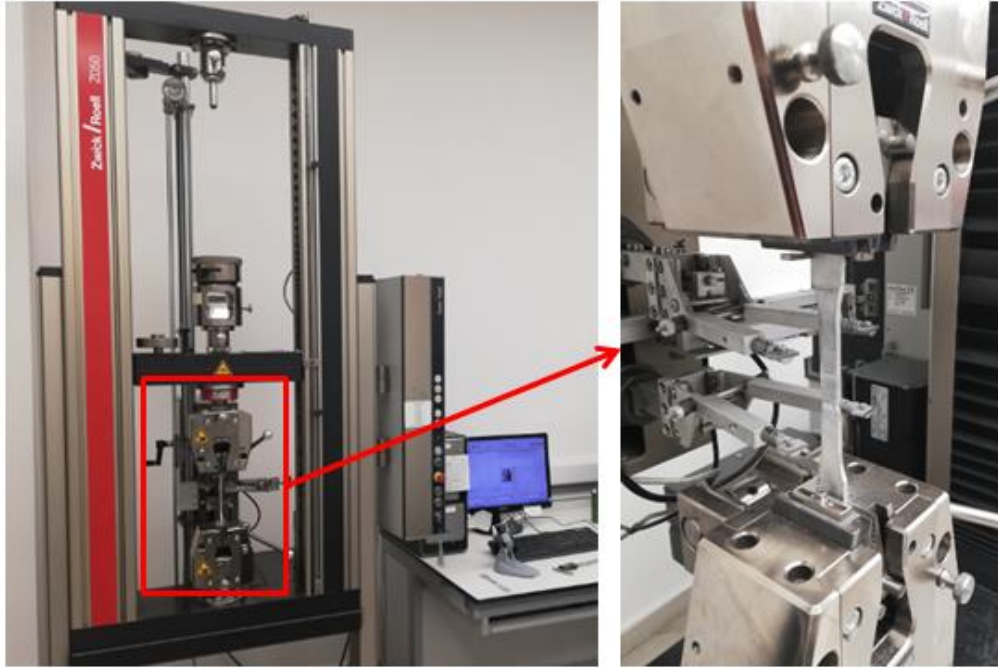
Figure 4.4: Universal tensile testing machine Zwick/Roell Z050

The dimension for the tensile specimen is given in Figure 4.5. The specimens were cut to the size of the standard tensile specimen with the help of special punching press having the dimensions of the tensile specimen.

All dimensions are in mm
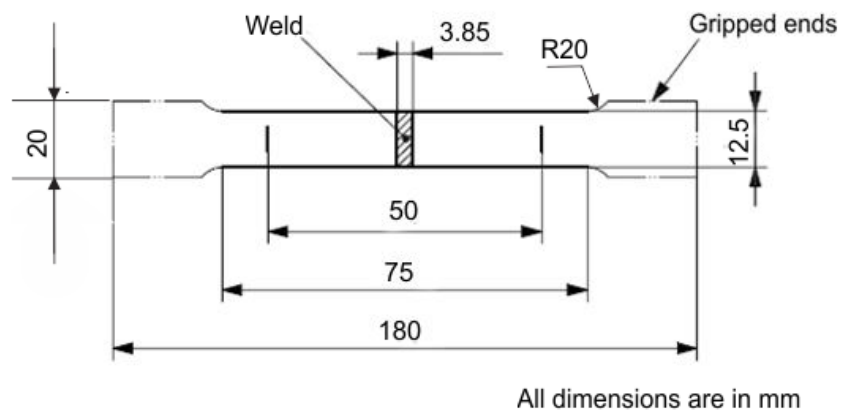
Figure 4.5: Tensile test specimen

For dissimilar welding specimens from specimen 1 to specimen 9, and specimen 18 and 19, and for similar welding of AA 6082, from specimen 14 to specimen 17, three tensile specimens are prepared for each number of specimens.

The average and the maximum tensile graphs are shown in Figure. Moreover, the efficiency of the weld is calculated according to equation 1.

$$Weld\ efficiency = \frac{\sigma_{joint}}{\sigma_{base\ metal}} \qquad \text{(Eq. 1)}$$

As given in the equation 1, weld efficiency is determined by the division of tensile strength of the welded joint to the tensile strength of the base metal. In case of dissimilar material welding, the material with lowest tensile strength is included in the equation. In this study AA 6005 having tensile strength of 270 MPa and AA 6082 having tensile strength of 290 MPa were welded; thus, for the calculation of the weld efficiency for dissimilar welding tensile strength of AA 6005 was taken into consideration.
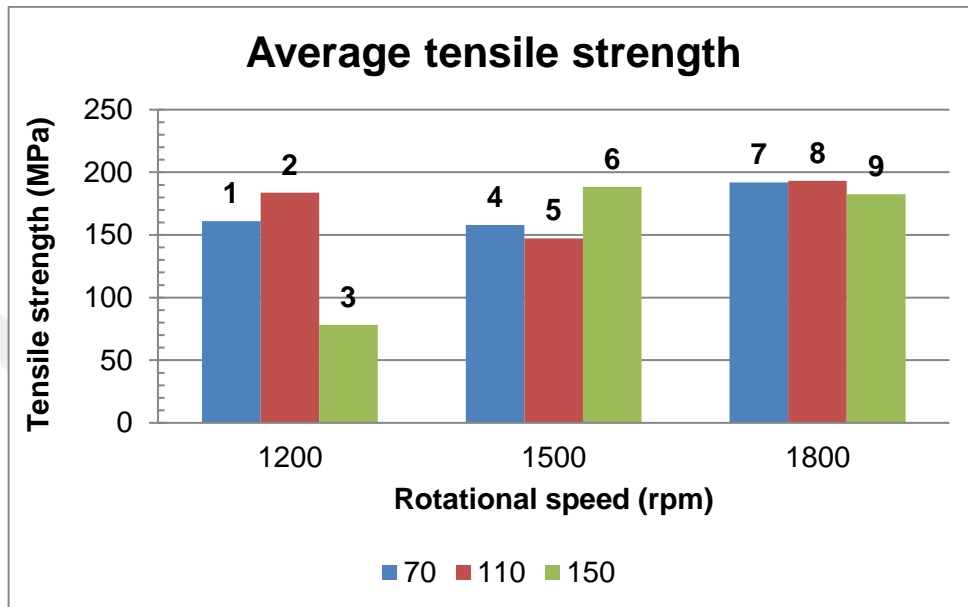
Figure 4.6: Average tensile strength for dissimilar welding
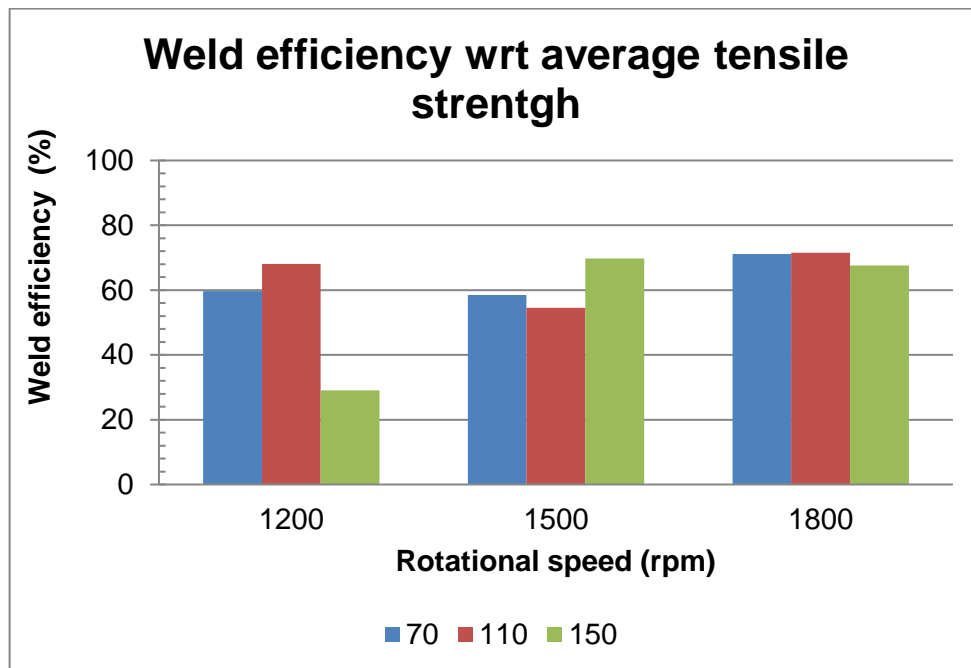
Figure 4.7: Welding efficiency with respect to average tensile strength for dissimilar welding

The average values from tensile test are given in Figure 4.6, it can be observed that the best results were obtained from the rotational speed of 1800 rpm, the efficiency of the weld is

above 60% for each welding speed at 1800 rpm as shown in Figure 4.7; however, the results did not show a trend at average values; thus, it is very difficult to comment on the effect of the parameters on FSW process.
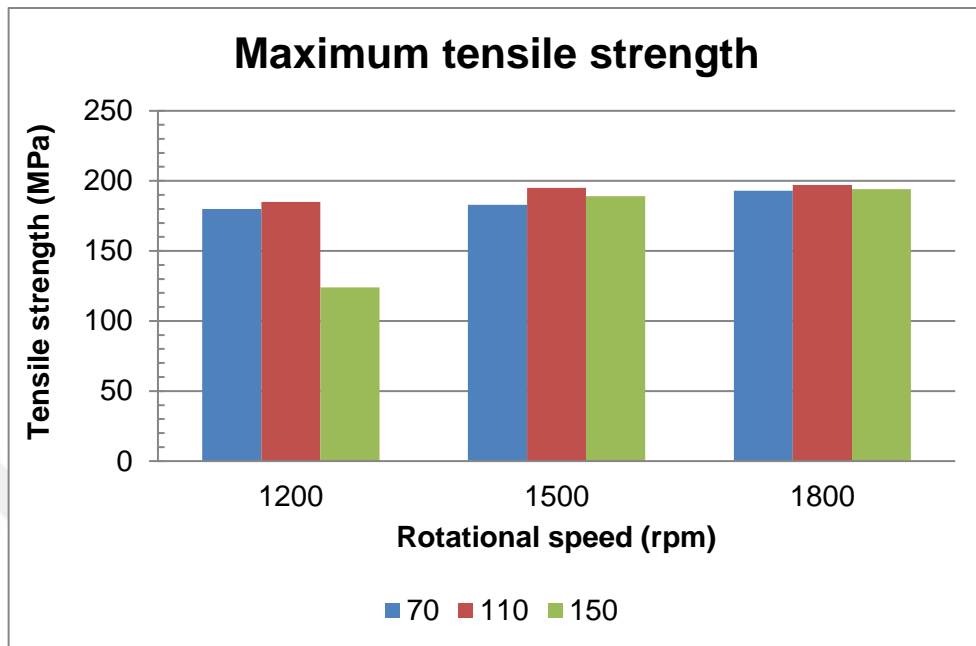
Figure 4.8: Maximum tensile strength for dissimilar welding

Moreover, the results from the average values and maximum values of the tensile strength, which can be seen in Figure 4.8, are quite different from each other, the reason is that specimens having void defects had quite lower tensile strength than the flawless specimens, also the void defect was observed to be discontinuous throughout the weld line since varied results obtained within the same specimens.
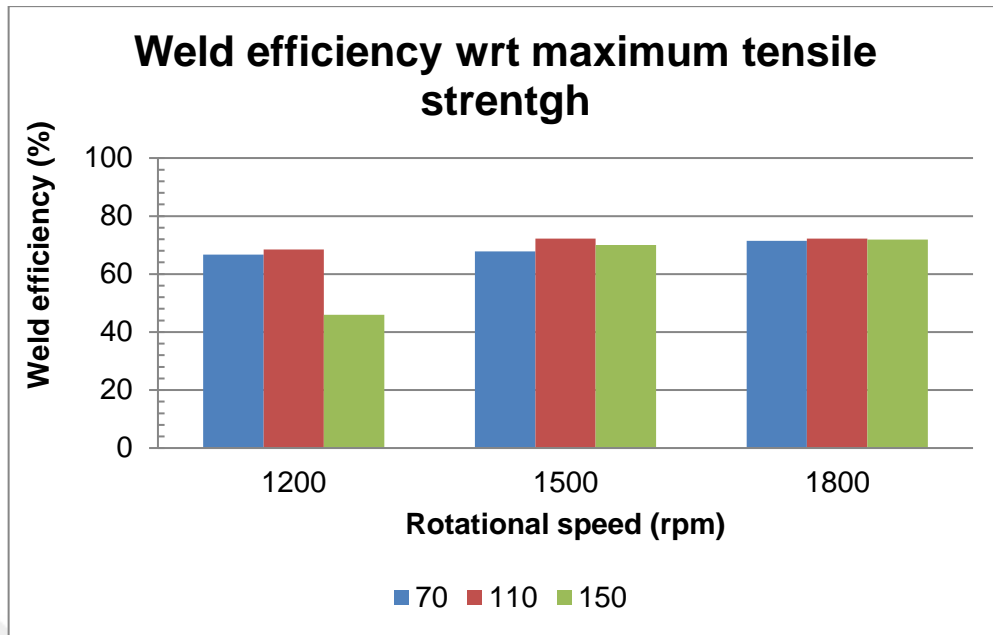
Figure 4.9: Welding efficiency with respect to maximum tensile strength for dissimilar welding

Welding efficiency with respect to maximum tensile strength for dissimilar welding is shown in Figure 4.9.

For example, in Figure 4.10 (a) and (b), the tensile test samples from the same specimen, specimen 9, are illustrated; even though, the samples were taken from the same welded plates, specimen (a) cracked just after passing the yield point at the region where void defect was present (TMAZ), whereas specimen (b) was cracked at heat-affected zone (HAZ) and did not fracture just after yield point like specimen (a).
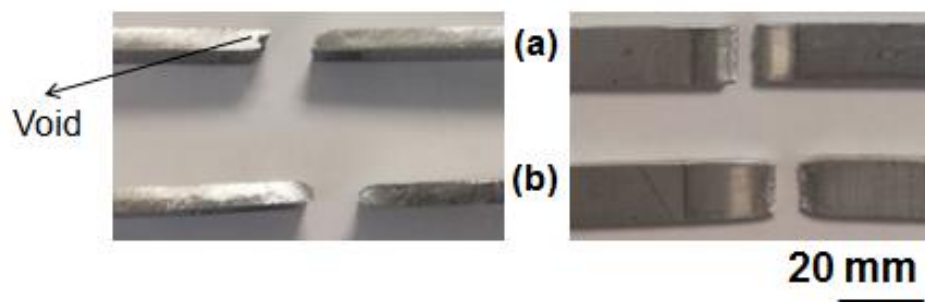
Figure 4.10: Fracture in the tensile specimens (a) at SZ from void defect, (b) at HAZ

Therefore, it is suggested that the results of the maximum tensile strength give more accurate results for the comparison of the process parameters and it is more convenient to take the maximum tensile strength values into consideration for commanding on the effects of the parameters on tensile strength

As shown in the graph, it is obvious for all specimens that when the rotational speed increases, the tensile strength increases at each constant welding speed. Moreover, the best results at each rotational speed were obtained at a welding speed of 110 mm/min.

The test results for welded AA 6005 plates were illustrated in Figure 4.11. As it can be seen from the graph, best result, 189 MPa was obtained at 1500 rpm and 110 mm/min with 70.1 % weld efficiency, minimum strength was obtained at 1500 rpm and 150 mm/min.
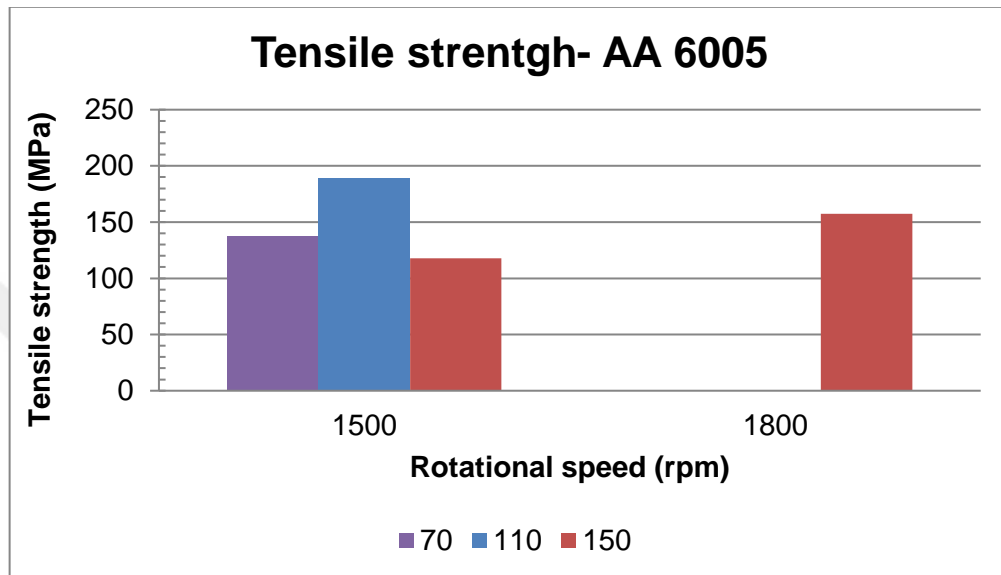
Figure 4.11: Tensile strength for AA 6005

The test results for AA 6082 are illustrated in Figures 4.12 and 4.13, the highest tensile strength was again obtained at 1500 rpm and 110 mm/min at both average and maximum tensile values, a maximum tensile strength of 212 MPa was obtained with 73.1% weld efficiency for specimen 15.
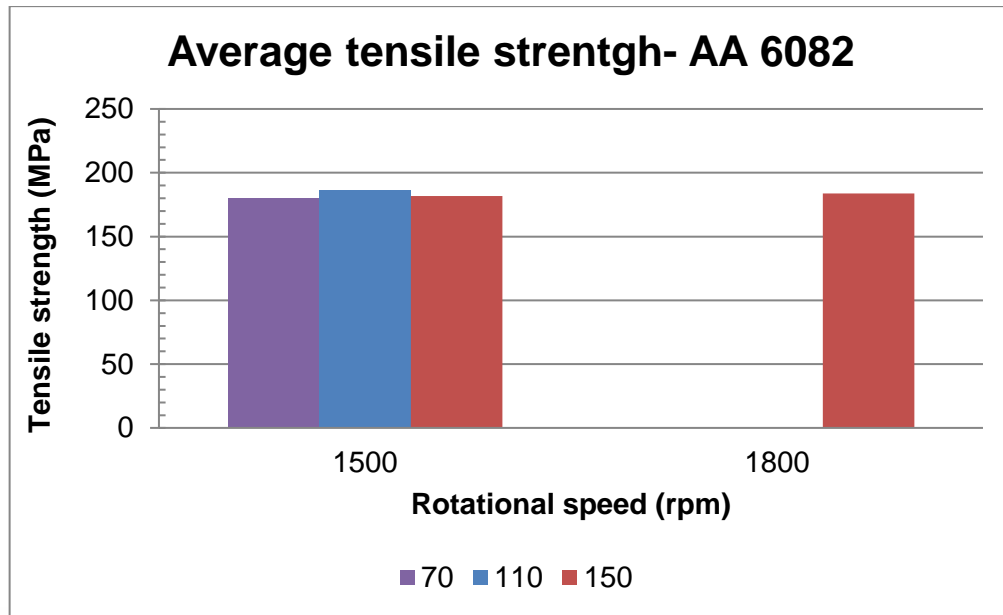
Figure 4.12: Average tensile strength for AA 6082
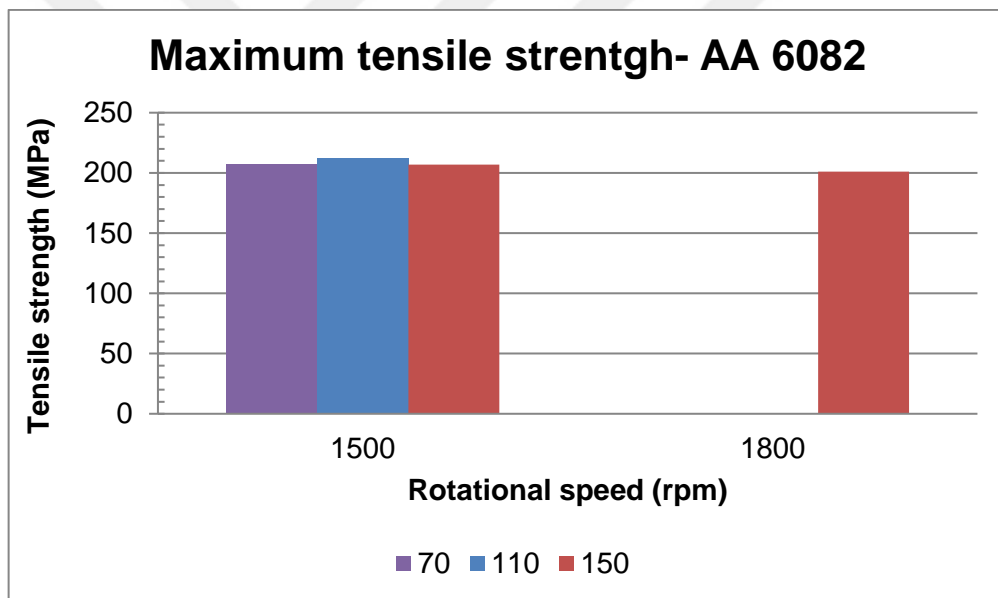
Figure 4.13: Maximum tensile strength for AA 6082

4.2 Macrostructural Analysis

Macrographs were taken by Nikon SMZ 745T stereomicroscope, the same etched specimens, which are prepared for microstructural analysis, were used in the macroscopic analysis. For the dissimilar welding between AA 6005-T6 and AA 6082-T6, the specimens numbers are from one to nine are shown in Figure 4.14.
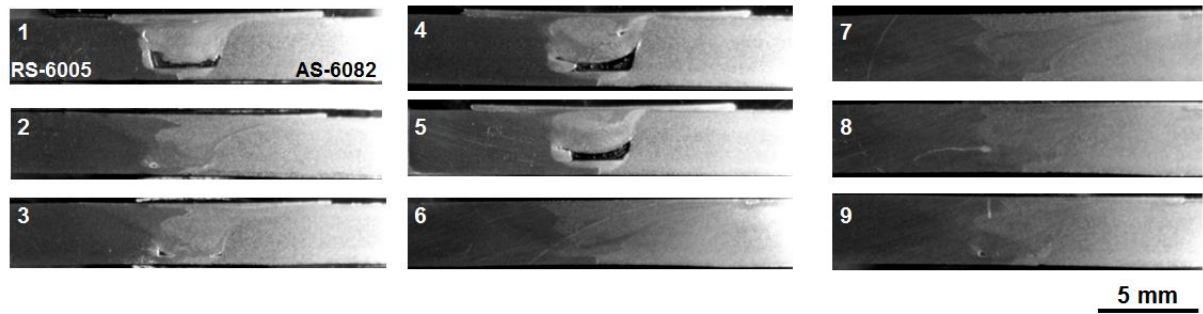
Figure 4.14: Macrographs for dissimilar welding

Severe void defects were observed at the specimen 1, 4, and 5. Also small voids are detected at the specimen 2, 3 and 9. There can be several causes for this kind of defect; however, as it can be seen from the micrographs when the rotational speed is increased to 1800 rpm in specimen 7, 8 and 9, the voids disappeared; thus, it can be said that one of the primary reasons for this kind of defect is insufficient heat input since as the rotational speed decreases the heat input decreases and the necessary heat for the flow of the material could not be obtained, and voids as a result of inadequate material flow. Another distinguishable defect is incomplete root penetration; in other words, lack of penetration. Specimen 1, 4 and 5 show clearly this flaw. Geometric defects such as lack of penetration defect, different from flow-related defects, occur as a result of inaccurate tool/joint adjustment/placement due to either mistaken pin length with respect to workpiece thickness or operator error [Loh10]. However, in this study, the pin length is designed with consideration of several other studies from the literature; the length of the pin was 0.2 to 0.3 mm shorter than the workpiece thickness.
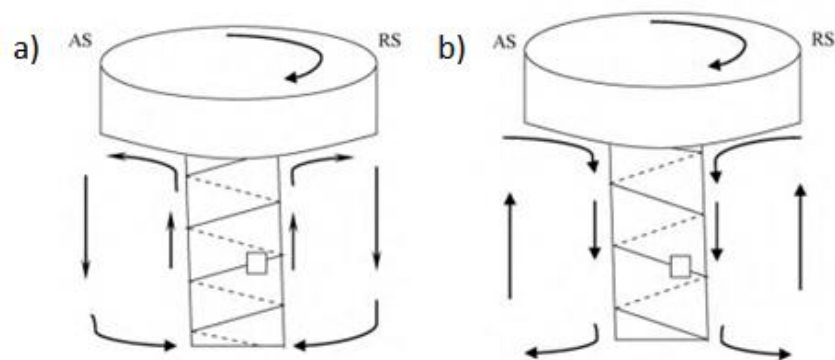
Figure 4.15: Material flow in FSW a) Right-hand thread and b) Left-hand thread pin tools in the clockwise rotation [Che10]

When it is assumed that the operator error was not present in the process, another suggestion as a reason for this defect is proposed, and that is the flow direction of the material resulting from the combination of the orientation of the pin threads and rotation orientation of the tool

As illustrated in Figure, for this study the flow behavior is the same as figure a) since the tool pin used in this study has a left-hand thread and the tool rotated in the counterclockwise, which causes the material to flow upwards and creating together with insufficient heat input the voids and incomplete root penetration effect.
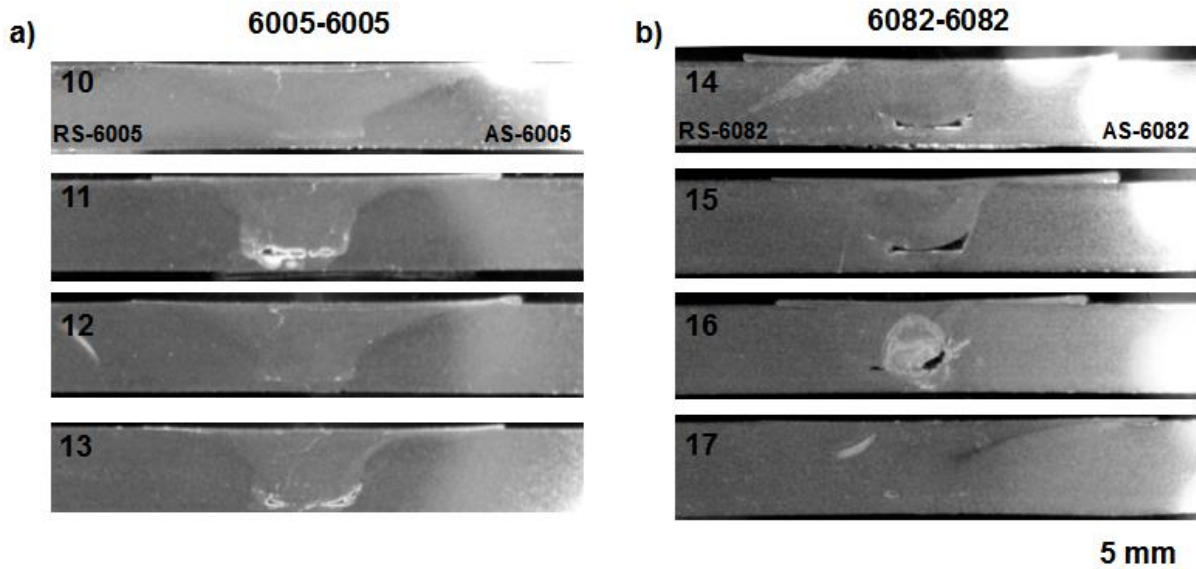
Figure 4.16: Macrographs for similar welding (a) AA 6005, (b) AA 6082

The macrographs from the similar friction stir welding of 6005 (a) and 6082 (b) are shown in Figure 4.16. The voids are smaller than in the dissimilar welding; however, for most of the parameter sets they are observable. The best result for 6005 aluminum alloy was obtained with specimen 10 without any distinguishable weld flaws whereas the best result for 6082 aluminum alloy was accomplished with specimen 17 only with small void at the retreating side(RS) of the weld. From the results it is difficult to make generalizations for the welding speed, and rotational speed since no trend followed by specimens was observed. It should be also noted that the void flaw is thought to be discontinuous throughout the weld seam for all of the specimens; therefore, it is not accurate to make a judgment on the weld properties only by macrograph results. However, it is obvious that there is relation between heat input, material flow, and void formation.

At the final batch of the experiments, rotational speed and welding speed were kept constant, 1500 rpm and 150 mm/min, respectively. The tilt angle is increased from 2° to 3° from specimen 6 to specimen 18. As seen in Figure 4.17, when the tilt is increased, the flash and void formation occurred; also the lack of penetration effect is increased. It was determined that when the tilt angle increases as the tool plunge depth are kept constant, the allowance for the upward material flow through the increased gap between workpiece and tool shoulder increases; thus, flash and void formation observed at the specimen 18.
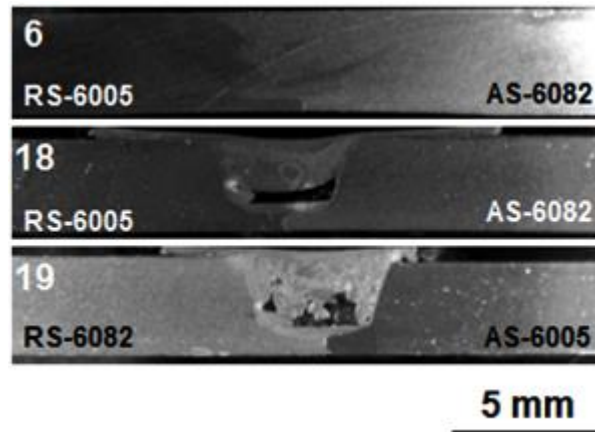
Figure 4.17: Macrographs for specimens with other parameter sets apart from rotational speed, welding speed including tilt angle and weld position

In this study, softer metal, 6005, was always placed at the retreating side (RS), and 6082 was placed at the advancing side of the weld. In order to see the effect of the weld position for the dissimilar friction stir welding, at the specimen 19, 6082 was located at the retreating side of the weld with keeping the other parameters same as specimen 6. When 6082 was placed at the retreating side of the weld, the flash mainly forming on RS of the weld observed; in addition, void formation and lack of penetration defect could not be avoided at specimen 18.

In addition, it can be observed from the macrographs that specimens of the dissimilar welds are clearly detectable as a result of different reactions of the dissimilar materials to the etching process. Also, from Figure 4.17, the difference between specimen 6 and 19 is observable; 6082 is brighter whereas 6005 has darker color.

In order to see and interpret the effects of the welding parameters in a more detailed and accurate way, further analysis with microscopic analysis and mechanical tests were done.

4.3   Microstructural Analysis

The microstructural specimens were cut to the smaller dimensions. After that, mechanical grinding was done using Silicon carbide (SiC) abrasive papers with different grit sizes of 180, 320, 500, 1200, 2400 grit respectively. In next step, the specimens were polished mechanically in two stages: Rough and final polishing with 9μm and 3μm colloidal silica (SiO_2). At last step, the specimens were electrolytic-etched with 12.5 V in 14 ml tetra fluoric acid in 700 ml water acid solution for 150 seconds. The steps are shown in Figure 4.18.

Figure 4.18: Preparation for the microstructural analysis

4.3.1 Analysis with Optical Microscopy

Microstructural analysis was done with an optical microscope, Zeiss Axio Scope A.1. The analysis was done in certain regions of the welded joint. Figure 4.19 shows the typical weld zones in FSW process. The micrographs were taken from those regions: Nugget zone (A), thermos-mechanically affected zone (B) and heat-affected zone(C).

A: Nugget Zone
B: TMAZ-Thermo-mechanically affected zone
C: HAZ – Heat affected zone
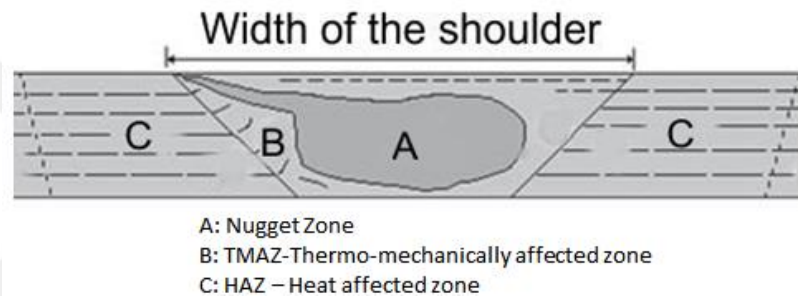
Figure 4.19: Regions of the weld for micrographs [Mis07] [Kum15]

The micrographs were shown in Figures 4.20- 4.25, in general, all regions can be detectable through micrographs. At stir zone (SZ) fine equiaxed grains were formed as a result of dynamic recrystallization. At lower welding speeds (70 mm/min and 110 mm/min) at 1200 rpm and 1500 rpm, onion ring-like structure was observed at SZ. Khodir and Shibayanagi have reported that onion ring patterns were identified by bands of varied sizes of the grain and non-uniform scattering of the alloying elements in stir zone independent of welding speed and position of the plates [Kho08]. HAZ region of AA6082 material has similar grain texture, fibrous grain structure, as the base material as expected. TMAZ region was more distinguishable at advancing side of the weld. It is identified by an extensively deformed structure with elongated grains in a shape of upward flow [Mis05]. The interface between TMAZ and HAZ are sharper, and TMAZ region is narrower in lower welding speeds as seen in specimens 1, 4, and 5. Bended grains in TMAZ due to plastic deformation observed more at higher welding speeds. In TMAZ region, fully recrystallization does not occur due to insufficient plastic strain. Mishra and Ma [Mis05] reported that in spite of experienced plastic deformation in TMAZ, it does not recrystallize due to inadequate deformation strain.

Zhao et al. [Zha05] related the distinct boundary between TMAZ and SZ with the insufficient flow of material and higher levels of speed. The sharp boundary between TMAZ and SZ can

be resulted here as well insufficient material flow at lower rotational speed (1200 rpm and 1500 rpm) since the sharp interface between two region disappeared at highest rotational speed (1800 rpm) due to higher heat input and improved stirring action and flow of material as shown in Figure.
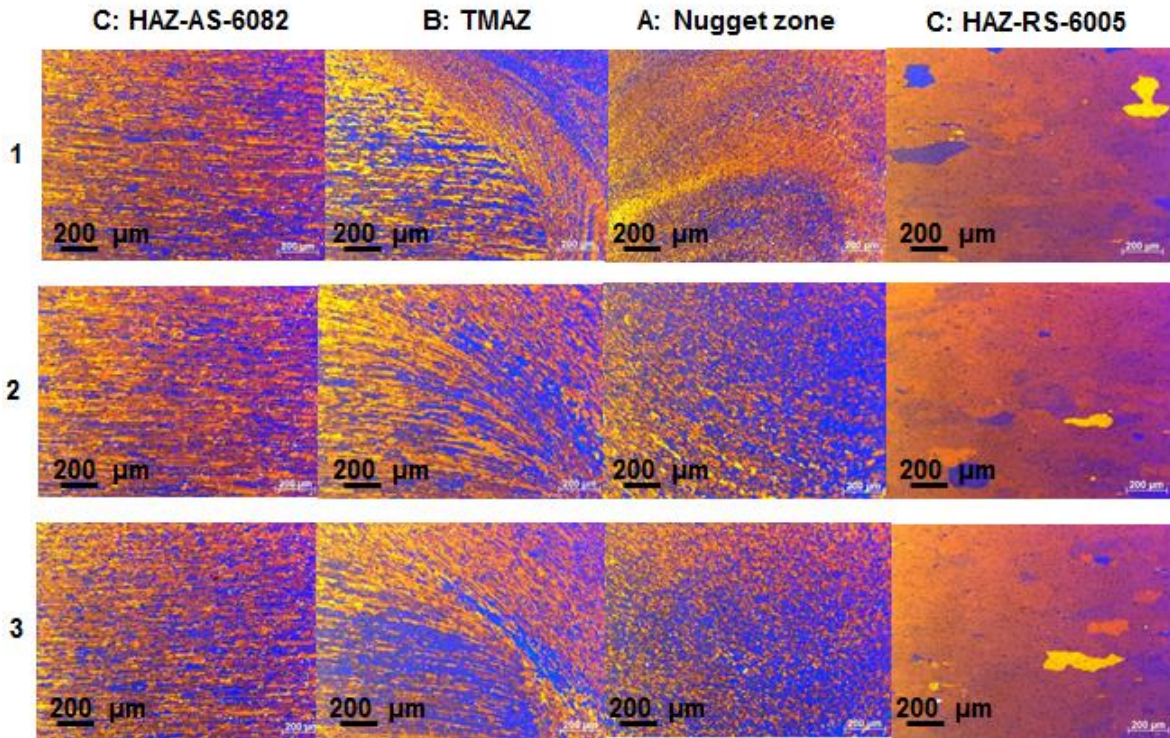
Figure 4.20: Micrographs for specimen 1, 2 and 3
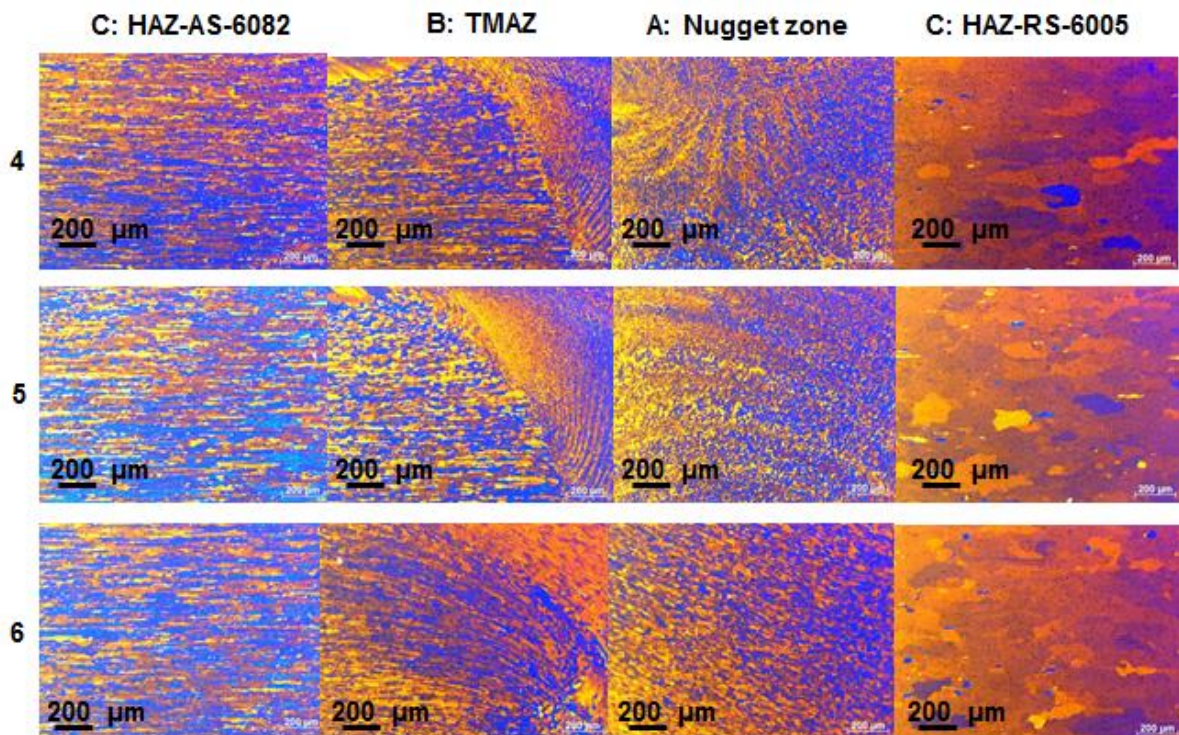
Figure 4.21: Micrographs for specimen 4, 5 and 6
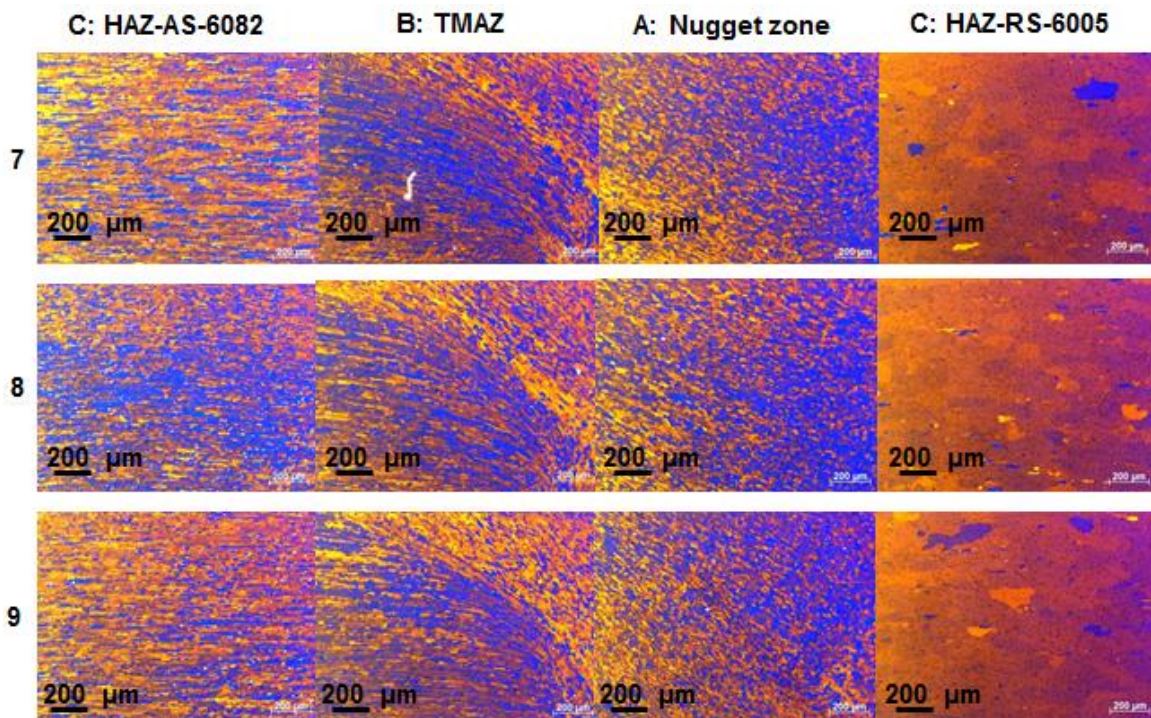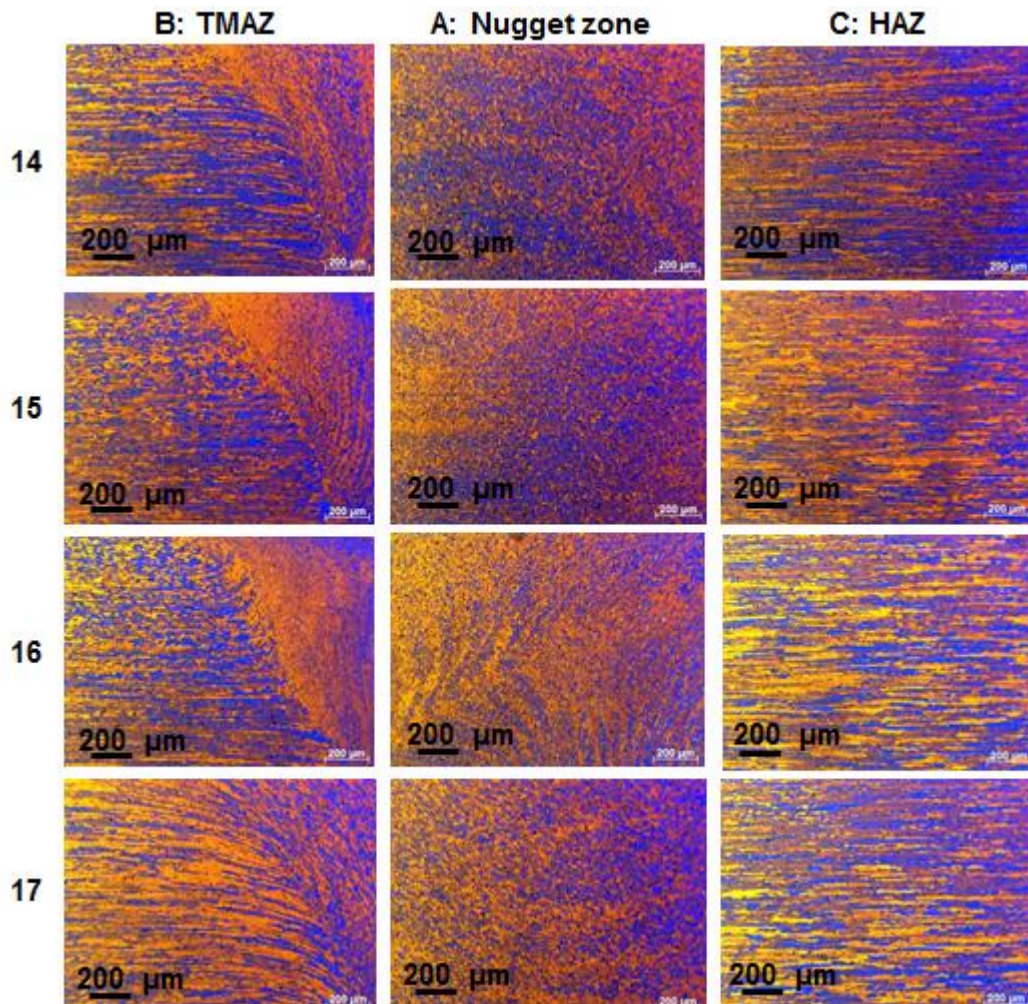
Figure 4.22: Micrographs for specimen 7, 8 and 9
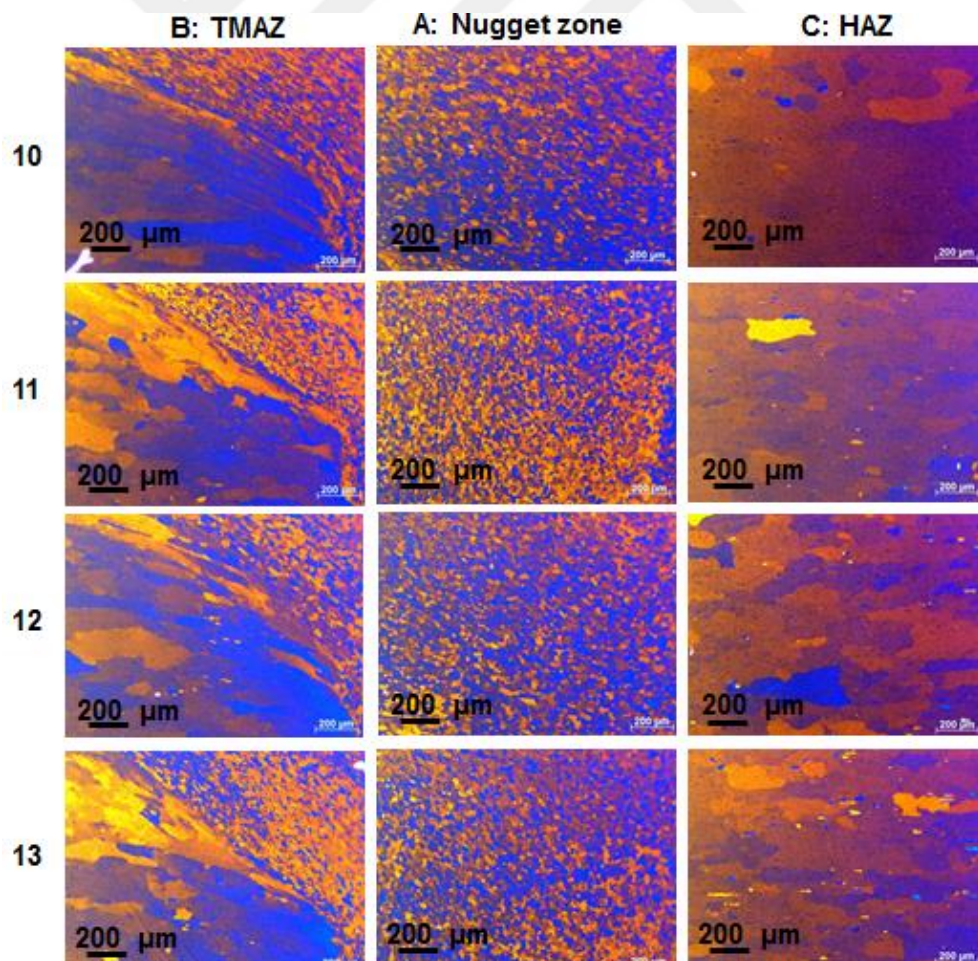
Figure 4.23: Micrographs for specimen 10, 11, 12 and 13

HAZ region of AA6005 at the retreating side has finer grains as the rotating speed increased as shown in Figure 4.22.

The size of the grains did not show distinctive change with rotational speed and welding speed in the first nine specimens. In similar welding of AA 6005 from specimen 10 to specimen 13 and AA 6082 from specimen 14 to specimen 17, as the welding speed increases at a constant rotational rate, the size of the grains gets smaller as a result of higher plastic deformation in a shorter time and lower heat input.

Figure 4.24: Micrographs for specimen 14, 15, 16 and 17

In order to see the effect of tilt angle, the comparison of the specimen 6 and specimen 18 were made in Figure, in specimen 18 when the tilt angle is increased with constant plunge depth, the boundary between SZ and TMAZ become more distinctive as a result of insufficient flow of the material and SZ shows onion ring pattern in specimen 18. Grain size in SZ decreased when the tilt angle increased as in the specimen 18. Furthermore, the effect of the position of the plates was analyzed in the study, AA 6005 was placed in the advancing side of the weld in specimen 19, as it can be seen from Figure, the void defects in nugget

zone were unavoidable under these welding conditions. Moreover, it was observed that when AA 6005 plate was fixed in the retreating side, mixing of the two materials was poor.
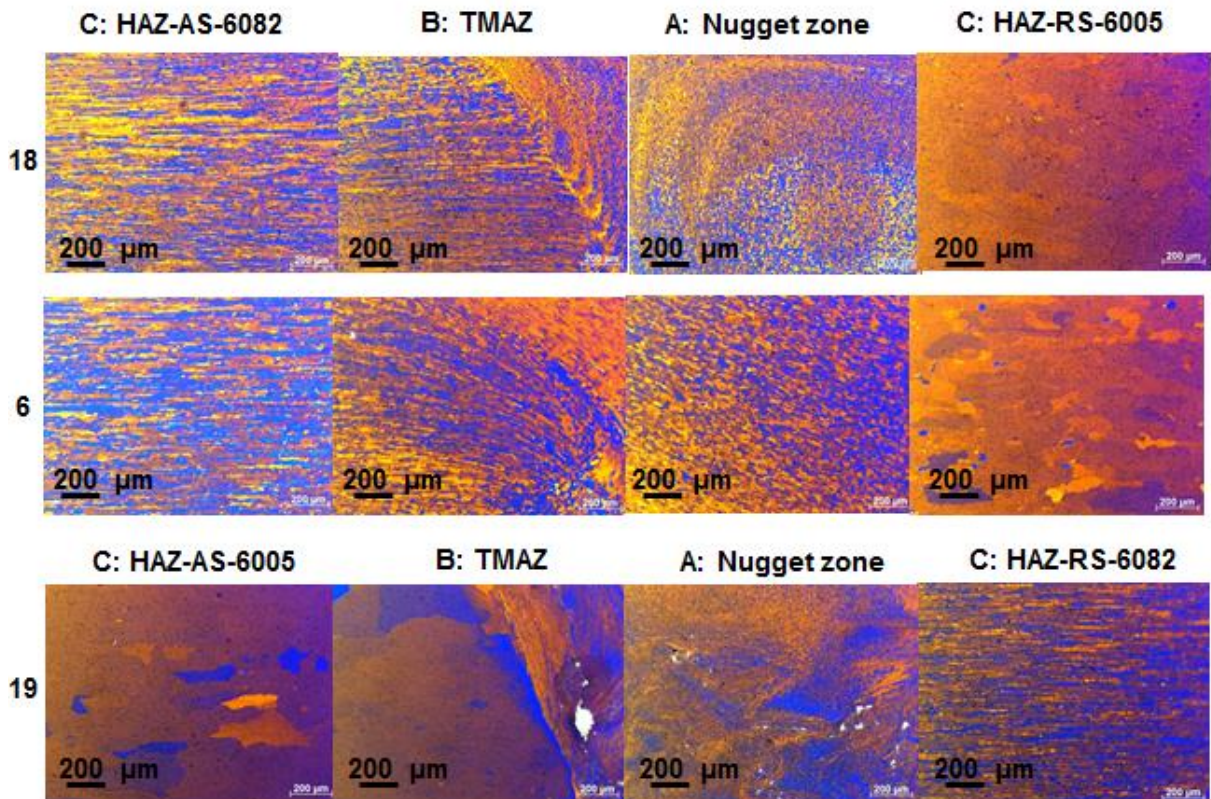
Figure 4.25: Micrographs for specimen 18, 6 and 19

4.3.2 Analysis with Scanning Electron Microscope (SEM)

SEM analysis was carried out with Zeiss EVO MAT 15 scanning electron microscope as shown in Figure 4.26(a) for the dissimilar welding specimens from specimen 1 to specimen 9 in order to analyze the second phases in the weld zone to make more accurate comments on the micro-hardness results.

Figure 4.26: (a) Scanning electron microscope (SEM) and (b) Gold plating process prior to SEM

The specimens which were utilized in optical microscopy analysis were used in the SEM analysis. In order to obtain better vision in SEM, previously etched specimens were mechanically ground with finest abrasive SiC paper of 2400 grit, later they were polished roughly and finely. The polished specimens were coated with gold as the last preparation step prior to analysis as shown in Figure 4.26(b).
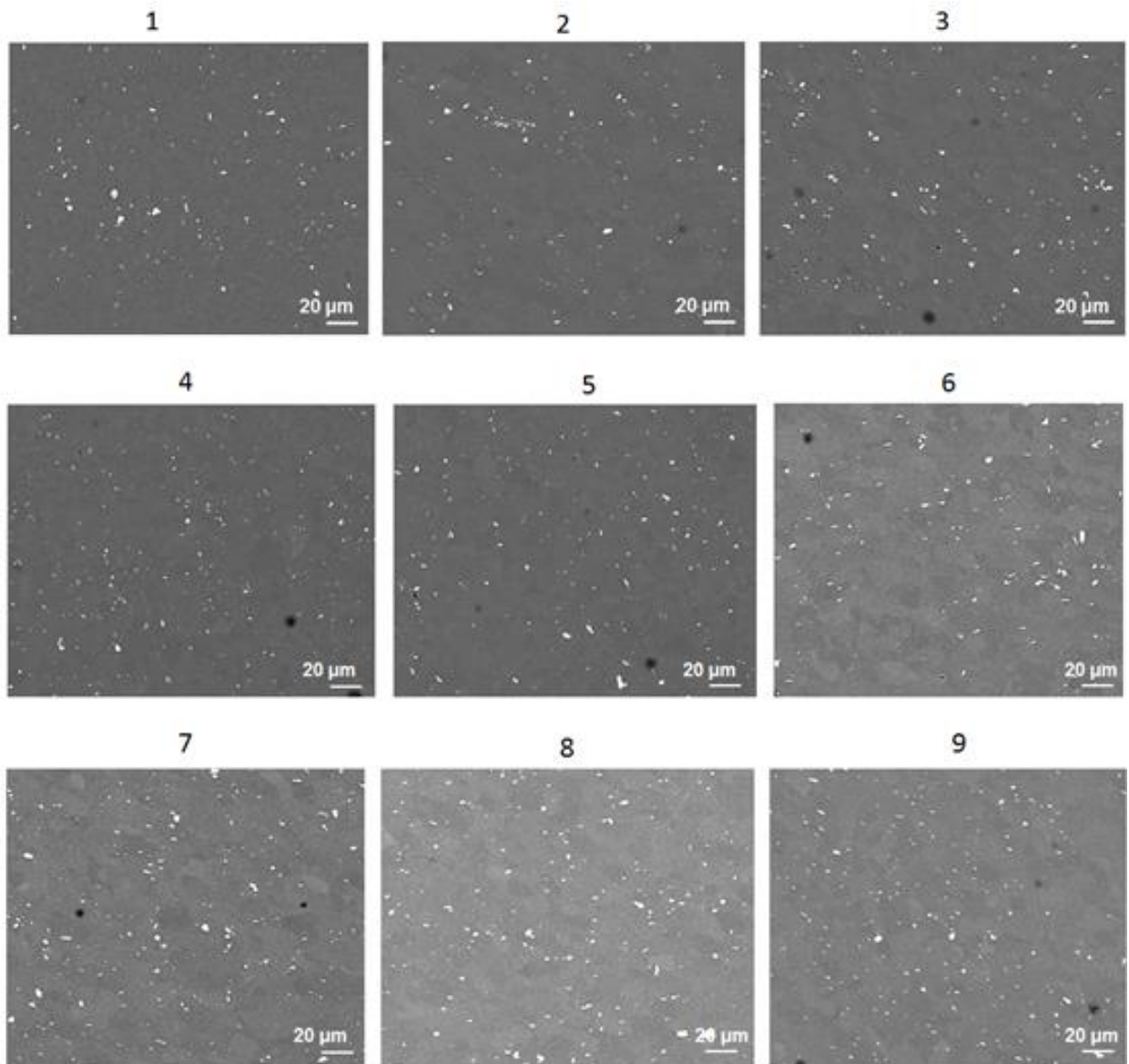
Figure 4.27: SEM images for dissimilar welding from specimen 1 to specimen 9

The working distance (WD) was 10 mm throughout the analysis; electron high tension (EHT) was set to 15 kV. The images were taken at a magnification of 1.00 KX at nugget zone in the weld. The precipitates seen in Figure 4.27 as white spots are analyzed through EDS (Energy Dispersive X-ray Spectroscopy) as stated in the next topic, and it was found out that the observable particles were intermetallic second phases existing in aluminum alloys in normal condition. Apart from strengthening precipitates, those intermetallic compounds have also effect on mechanical properties of the aluminum alloys. It is clear that when the specimen 3,

6 and 9 are observed, it is seen that the size of the intermetallic phases decreases with increasing rotational speed in spite of hotter weld conditions as a result of increased plastic deformation through stirring action. Moreover, it can be observed that as the welding speed increases the size of the precipitates usually decreases as a result of colder weld conditions.

EDS Analysis
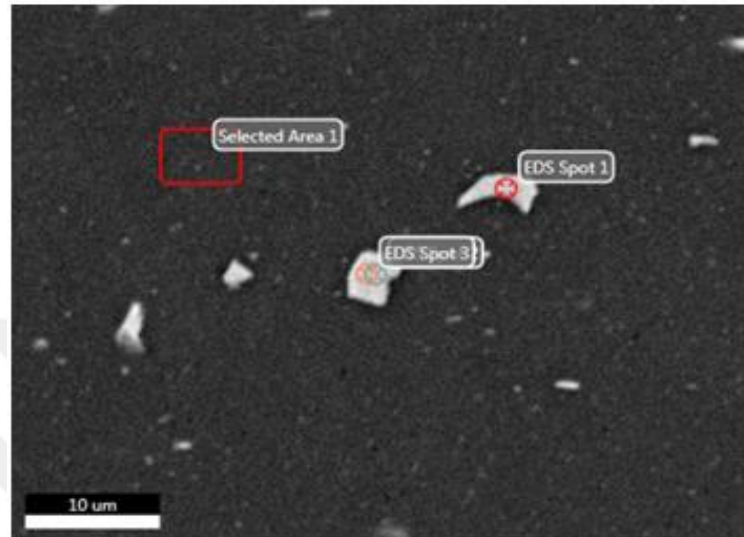
Figure 4.28: Selected region for EDS analysis

EDS analysis was carried out in order to see the composition of precipitates as seen in Figure 4.28. It was observed that white-colored precipitates existing in the Fe-, Mn-, Si-, and Cr-based second phases, listed starting from the highest composition, normally existing in the aluminum alloys. Strengthening precipitates such as Mg_2Si is not observable through SEM; for this purpose, more detailed analysis should be carried out through TEM (Transmission Electron Microscopy) in order to see the effect of the precipitates on mechanical properties such as micro-hardness and tensile strength.

Compositions of the three spots from the figure are shown on Table and the graphs in Figures 4.29- 4.31.
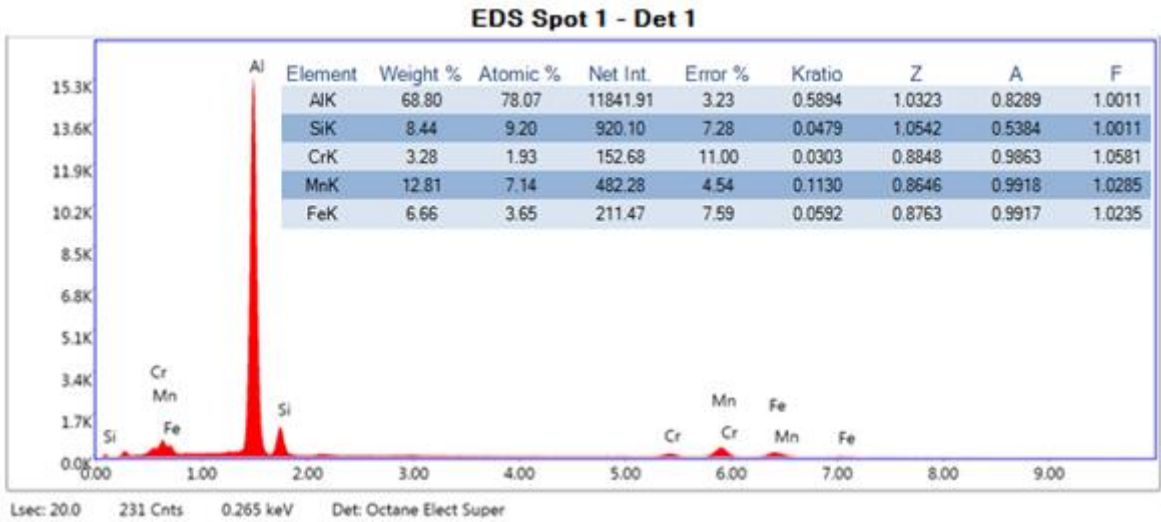
Figure 4.29: Composition for EDS Spot 1
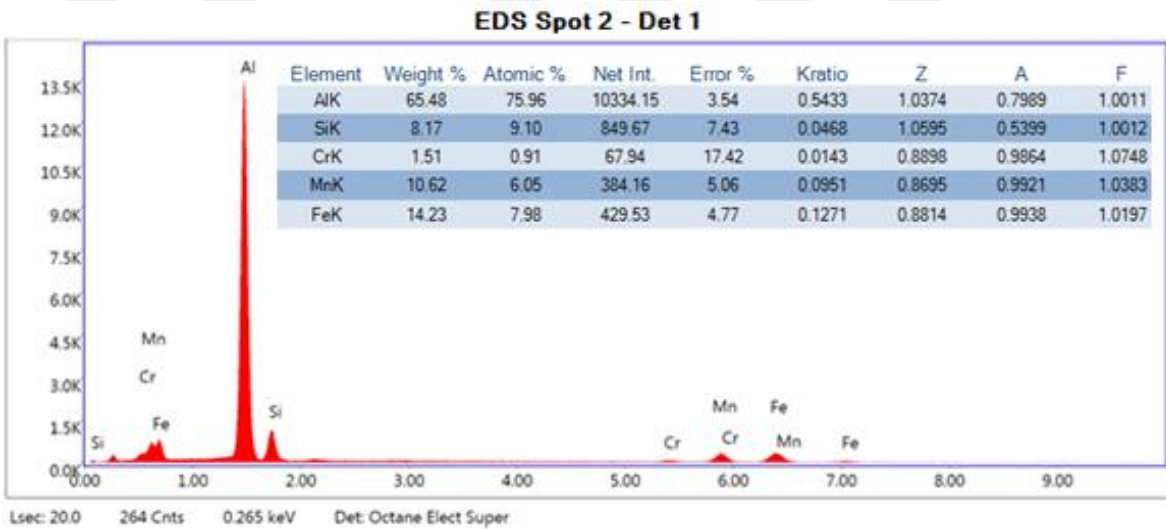
Figure 4.30: Composition for EDS Spot 2
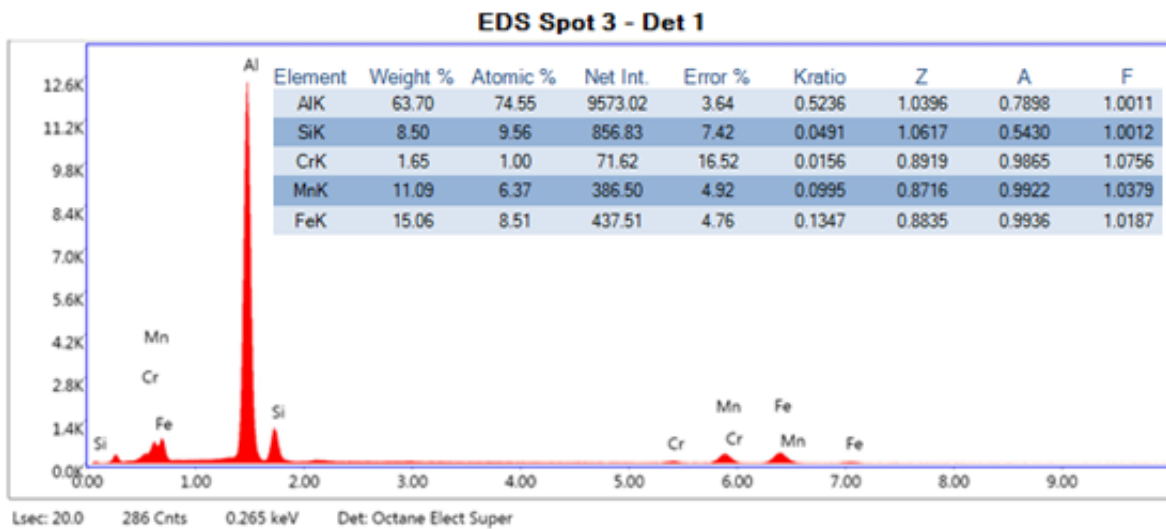
Figure 4.31: Composition for EDS Spot 1

4.4 Microhardness Test

In order to make more accurate and sound comments on the quality and effects of parameters in the welding process, the tensile test results are not sufficient itself; thus, for better interpretation of the results micro-hardness test is required. Microhardness measurements were conducted with Future-Tech FM-700 microhardness tester. Applied test load was 100 gf, and the force is applied for 10 seconds.
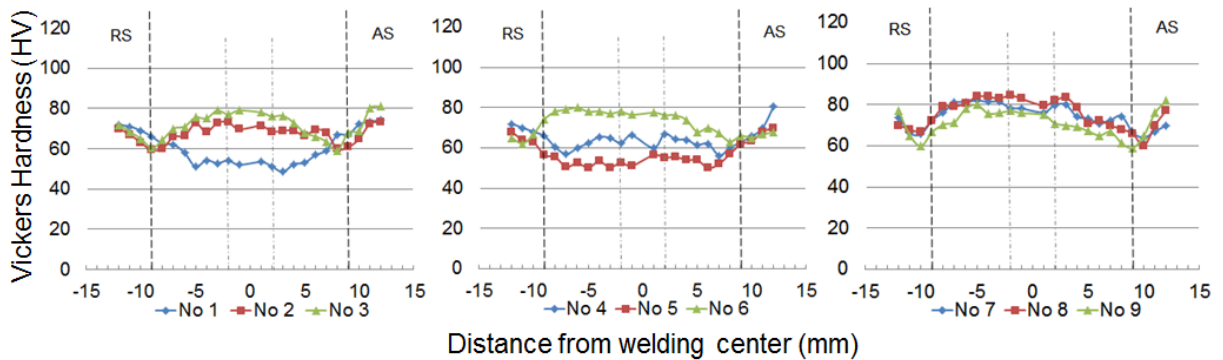
Figure 4.32: Microhardness graphs classified with constant rotational speed for dissimilar welding
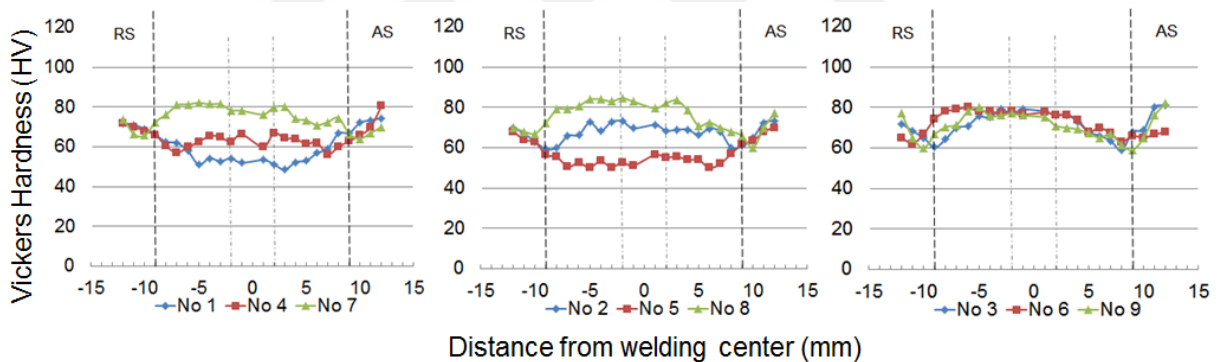
Figure 4.33: Microhardness graphs classified with constant welding speeds for dissimilar welding

Vickers hardness values were measured within the ±12 mm from the weld center line with 1 mm distance between each indentation. In Figures 4.32 and 4.33, the sets of graph according to their welding speed and rotational speed are given, respectively, for the first nine specimens. First of all, it should be noted that the specimens show the W-shaped profile for the hardness distribution throughout the welding zones at each specimen. Hardness is expected to be decreased in HAZ for several possible reasons such as coarsening of the strengthening precipitates, over-aging or grain growth. In SZ, the hardness is higher than HAZ; however, it is lower than the hardness of the base metal, it is predicted that in SZ, hardening precipitates were firstly dissolved, and then precipitated again. For alloys in overaged or peak state (T6, T7, or T8), there will be typically reduced hardness area in HAZ as a result of coarsened precipitate distribution and overaging due to thermal transient

[Mis07]. In HAZ region, it is predicted that the precipitates were coarsened and the over-aging occurred, and the T6- T7 conditions are obtained due to thermal cycle exerted on the region. Many researchers also suggested similar explanations for the softening of HAZ and TMAZ region, which were coarsening and dissolution of the precipitates in 6xxx series alloys [Kha17].

In the first three specimens (1, 2, and 3) it can be seen that as the welding speed increases, the hardness also increases.

It could also be observed that as the rotational speed increases at constant welding speed, the hardness minima places further from weld center. In Figure, it is also noticeable that at 150 mm/min (specimen 3, 6, and 9), rotational speed lost its effect on micro-hardness. The similar situation is observed at the rotational rate of 1800 rpm since the hardness values are very close to each other in specimen 7, 8 and 9.
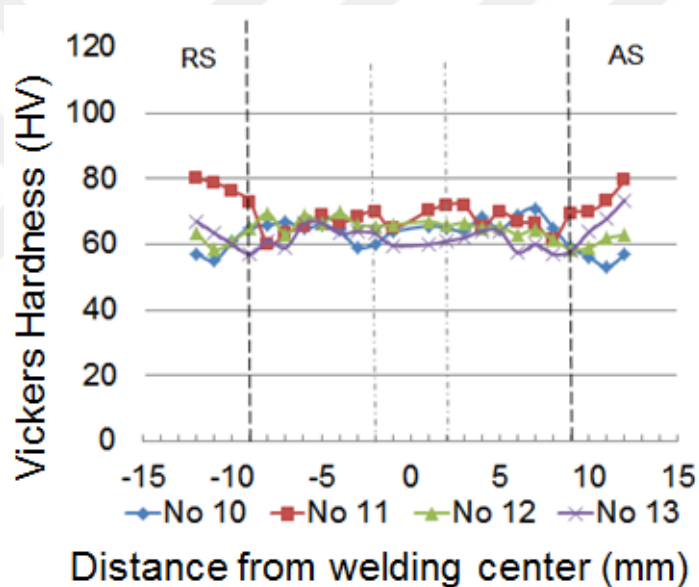
Figure 4.34: Microhardness values for similar welding of AA 6005

Even though the hardness values in FSW of AA 6005 are very close to each other in all specimens, it is still observable that highest value was obtained at specimen 11 where the rotational speed 1500 rpm and the welding speed was 110 mm/min as shown in Figure 4.34. The same processing parameters form the highest hardness values for AA 6082 as in specimen 15 as shown in Figure 4.35.
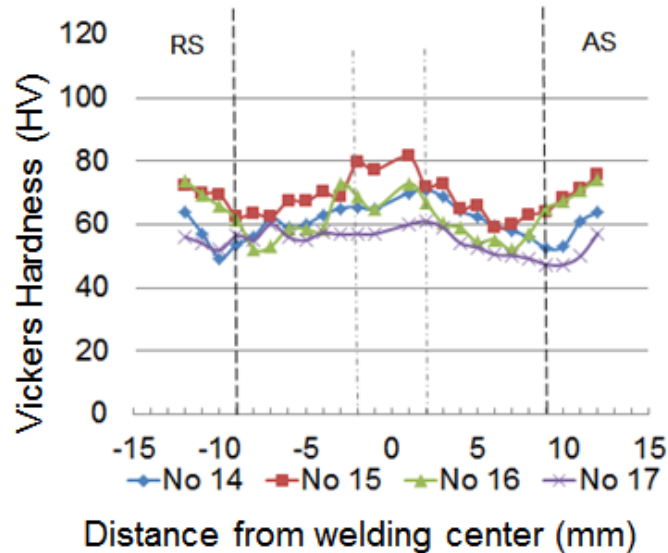
Figure 4.35: Microhardness values for similar welding of AA 6082

Process parameters apart from rotational rate and welding speed were changed in the specimens shown in Figure 4.36. Hardness value in SZ increases whereas the hardness gets lower values in TMAZ and HAZ region when the tilt angle increases in specimen 18. When the position of the plates is changed as in the specimen 19, the hardness minima in both sides of the weld was observed just after the SZ in TMAZ region instead of HAZ region as it is observed in other specimens except specimen 18. Furthermore, the hardness in SZ was observed to be decreased when AA 6005 is placed in the advancing side in specimen 19.
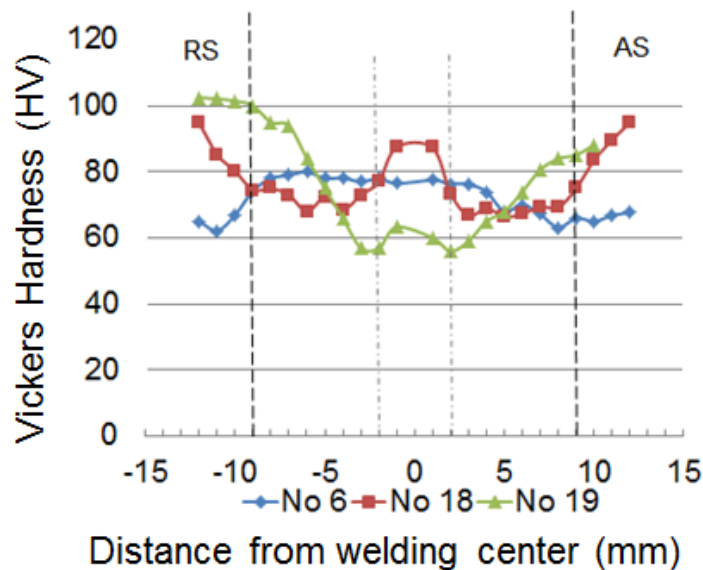
Figure 4.36: Microhardness values for third welding set including the effect of tilt angle and weld position

5 Discussion

In general, in the study, it is observed that tensile test results only does not provide a realistic evaluation of the weld quality; thus, microscopic analysis and microhardness measurements should be carried out.

In the case of FSWs of precipitation-hardening alloys, "W"-shaped distribution of hardness is typical [Mis07]. This distribution pattern was observed in this study in FSW of AA 6005 and AA 6082 alloys.

Li and Liu stated that when the welding speed increases gradually, the microhardness of TMAZ and HAZ increases because of restrictions in precipitate dissolution and grain growth as a result of less peak temperature and holding time [Li13]. Mishra and Mahoney stated that the faster weld shows higher hardness values in SZ and hardness minima in HAZ; moreover, in fast weld, the hardness minima is positioned further from weld centerline than in slow weld [Mis07]. At the rotational speed of 1200 rpm, it is observed that hardness increases with increasing welding speed; however, this trend could not be seen at other rotational speeds.

Mishra and Mahoney also reported that higher hardness in faster weld would give higher tensile strength in transverse direction than in slower weld [Mis07]. It is observable that the highest micro-hardness results correlate with the highest tensile strengths in specimen 8, 11 and 15 within the similar and the dissimilar weld sets. Li and Liu also concluded that tensile strength increases with increasing welding speed up to a certain value and then it starts to decrease; the least tensile strength was obtained at lowest welding speed due to growth in grain resulting from higher holding time and heat input [Li13]. Sakthivel et al. reported that hardness is increasing slightly with increasing welding speed; ultimate tensile strength increases with decreasing welding speed [Sak09]. In this study, it is generally observed that when the welding speed increases gradually, the tensile strength increases and then decreases with further increase in welding speed.

Khodir and Shibayanagi found out that tensile properties of the weld depend primarily on the defects in the weld and hardness of the weld joint; when joints are flawless, hardness controls the tensile properties, and fracture occurs in HAZ where the hardness is minimum [Kho08]. The same behavior was also observed in the FSWs of 6000 series aluminum alloys used in this study. Specimens with void defects were cracked from the void defects whereas defect-free joints were failed in the region of HAZ, where microhardness values were observed to be lowest throughout the measurement line. Tensile tests were conducted more than once for each specimen, and it was seen that the same parameter sets might result in quite fewer values than the maximum obtained value because of defected joints; therefore, it is suggested that when the joints are compared according to their process parameters, it will

be more accurate to compare the maximum tensile strengths within each specimen numbers. Average tensile strengths might give misleading results.

$$\sigma_{min,w} = \sigma_{min,pm} f_e \qquad \text{(Eq.2)}$$

In the equation 2 (Eq.2), the required minimum tensile strength is given, which is the multiplication of f_e, the efficiency of the connection, and $\sigma_{min,pm}$, the specified minimum tensile strength of the required base material, according to DIN EN ISO 25239-4 standard, f_e the value should be 0.7 for the artificially aged T5 and T6 conditioned alloys. Therefore, for this study, if the efficiency of the connection is equal or above 0.7 or 70% it is acceptable in terms of quality by the FSW standards. It was accomplished by specimens 5, 6, 7, 8, 9, 11, 14, 15 and 16.

Another significant outcome of this study is that even though it is noted in the literature that proper usage of the tool with left-hand thread tool pin requires clockwise rotation of the tool; it is observed that counterclockwise rotation gives successful results in terms of the appearance and quality of the weld bead.

6 Summary and Outlook

The aim of this study was to evaluate the 6000 series aluminum alloys and obtain the best optimum parameter sets for the provided test plan. For this purpose, AA 6005-T6 and AA 6082-T6 aluminum alloys were welded in three sets with main focus on the effect of the rotational speed and welding speed on the weld quality. These sets included dissimilar welding of AA 6005-T6 and AA 6082-T6, and similar welding of the alloys separately. The plates with a dimension of 200x90x3.9 mm are welded at 5-axis CNC machine, Mazak VTC-800/30SR; the fixture and tool design were done and manufactured. The tool material was selected as AISI-H13 steel which was subsequently heat-treated to improve its hardness to approximately 55 HRC. The fixture material was AISI-1050 carbon steel. The three levels of two parameters (rotational speed and welding speed) were accomplished in the welding of dissimilar set of experiments. For similar welding, two different rotational speed and three different welding speeds were applied during welding of similar materials. After the trials, macro- and microstructures were analyzed with Nikon SMZ 745T stereomicroscope; Zeiss Axio Scope A.1 optical microscope and Zeiss EVO MAT 15 scanning electron microscope, respectively. The tensile tests were carried out according to DIN EN ISO 6892-1 [DIN10] with universal tensile testing machine Zwick/Roell Z050 with the gauge length is 50 mm and the testing speed of 10 mm/min. The microhardness measurements were done with Future-Tech FM-700 microhardness tester with applied test load of 100 gf for 10 seconds.

For dissimilar sets of materials, from specimen 1 to specimen 3, hardness values were observed to be increased as the welding speed increases at a constant rotational speed. However, this trend was absent in the rest of the specimens. It is observed in FSW of dissimilar welding that hardness minima place further from weld center when the rotational speed increases at constant welding speed. The maximum hardness value in SZ was obtained in specimen 8 as 84.6 HV when the welding speed is 110 mm/min, and the rotational rate was 1800 rpm. The maximum tensile strength also observed in specimen as 197 MPa.

For the similar welding of AA 6005, the highest tensile strength was 189 MPa with process parameters of 1500 rpm and 110 mm/min with 70.1 % weld efficiency for specimen 11, the minimum strength was detected at 1500 rpm and 150 mm/min. For the similar welding of AA 6082, the highest tensile strength was seen with process parameters of 1500 rpm and 110 mm/min at both average and the maximum tensile values, maximum tensile strength of 212 MPa was obtained with 73.1% weld efficiency for specimen 15. The hardness values for similar welding are consistent with the tensile test results for similar welding of aluminum alloys. The maximum hardness reached to 72 HV in SZ in the welding of AA 6005 similar

alloys at specimen 11. Also, the maximum hardness in SZ of AA 6082 alloy was measured as 81.4 HV for specimen 15.

Void defects were observed in some specimens as the main result of inadequate material flow as a result of insufficient heat input. When void defects observed, the material fails at SZ in tensile test; otherwise, it fractured in the HAZ region. The tensile test results were evaluated according to DIN standards, which states that for the case of T5 anT6 artificially aged condition; the acceptable weld efficiency is at least 70%. In the study, some results above this limit obtained.

The parameters can be improved according to outcomes of this study; first of all, it is clear that cold welds lead in insufficient material flow, and accordingly, void formation. Therefore, when determining process parameters sufficient heat generation should be secured.

The tool used in this process was initially designed with left hand threaded pin tool since some of the previous studies recommended the use of left hand threaded pin with clockwise tool rotation; nonetheless, even though, trials with various parameters successful results could not be obtained with this combination; therefore counterclockwise rotation was preferred. Due to the upward flow of the material near tool pin, at the bottom of the weld defects causing from lack of penetration were observed. Therefore, for the future studies in case of the same combination as this study, pin length could be designed about 0.1 mm longer than the current pin length.

In case of improved tensile properties and weld quality, post-weld heat treatment could be applied in future studies.

Non-destructive testing methods such as radiography and ultrasonic test are highly recommended to be included in the testing plan in order to detect defects like porosity and voids throughout the welding line.

Another important parameter for FSW of dissimilar material is that tool offset towards one side of the weld, either on advancing side or retreating side. In this study, this offset value was out of focus, and the tool offset was set to zero. For improved welding quality, the tool offset value can also be investigated in the future works.

In order to understand the mechanism of the loss in mechanical properties, the strengthening precipitates apart from intermetallic second phases could be observed in detailed, the use of SEM is not sufficient for this purpose; therefore, TEM should also be utilized, or the other techniques such as measuring the temperature in the plates should be applied in order to detect the state of the precipitates.

7 References

[Abd18] Abd El-Hafez, H.; El-Megharbel, A.: Friction Stir Welding of Dissimilar Aluminum Alloys. World Journal of Engineering and Technology, 6, pp. 408-419, 2018

[Ais10] Aissani, M.; Gachi, S.; Boubenider, F.; Benkedda, Y.: Design and Optimization of Friction Stir Welding Tool, Materials and Manufacturing Processes 25 (11), 2010.

[Arb03] Arbegast, W.J.: Modeling friction stir joining as a metal working process, Presented at Hot Deformation of Aluminum Alloys III, San Diego, CA, USA, 2003.

[Ata03] Ataoglu, H., Mıstıkoglu, S., CAM, G., "Sürtünme Karıştırma Kaynaklı Bir Al-Alaşımının İçyapı ve Mekanik Karakterizasyonu", TMMOB Makine Mühendisleri Odası Kaynak Teknolojisi IV. Ulusal Kongre ve Sergisi, 65-75, Kocaeli, 2003.

[Bag12] Baghel, P. K.; Siddiquee, A. N.: Design and development of Fixture for Friction Stir Welding, Innovative Systems Design and Engineering Vol 3, No.12, 2012.

[Bia99] Biallas, G.; Braun, R.; Donne, C.D.; Staniek, G.; Kaysser, W.A.: in: Proceedings of the First International Symposium on Friction Stir Welding, Thousand Oaks, CA, USA, June 14–16, 1999.

[Cav08] Cavaliere, P.; Squillace, A.; Panella, F.: Effect of welding parameters on mechanical and microstructural properties of AA6082 joints produced by friction stir welding. Journal of Materials Processing Technology. 200:364–372, 2008.

[Cev12] Cevik, B.; Ozcatalbas, Y.; Uygur, I.: 7075 Alüminyum Alaşımının Sürtünme Karıştırma Kaynağı ile Birleştirilmesi, International Conference on Welding Technologies and Exhibition, Ankara, Turkey, 2012.

[Cha15] Chandrashekar, A.; Ajay Kumar, B. S.; Reddappa, H. N.: Friction Stir Welding: Tool Material and Geometry, Akgec International Journal Of Technology, Vol. 6, No. 1, 2015.

[Che10] Chen, D.; Cao, X.: Tensile properties of a friction stir welded magnesium alloy: Effect of the pin tool thread orientation and weld pitch, Materials Science and Engineering A 527(21-22):6064-6075, 2010.

[Col07] Colegrove, P.A.; Shercliff, H.R.; Zettler R.: Model for predicting heat generation and temperature in friction stir welding from the material properties, Science and Technology of Welding and Joining, vol. 12, 4, pp. 284–297, 2007.

[Cor88] Cornu, J.: Advanced Welding Systems: Fundamentals of Fusion Welding Technology, Springer-Verlag Berlin Heidelberg, p.11, 1988

[Bar00]   Barnes, T.A.; Pashby, I.R.: Joining techniques for aluminum space frames used in automobiles: Part I—Solid and liquid phase welding. Journal of Materials Processing Technology. p99:62–71, 2000.

[Bar12]   Barlas, Z.; Ozsarac, U.: Effects of FSW Parameters on Joint Properties of AlMg3 Alloy, Welding Journal (91), 2012.

[Dag16]   Dagdelen, E.; Ulus, A.: Aluminum Sheet Production: Heat Treatment of Aluminum and Temper Designations of Aluminum Alloys, TMMOB Metalurji ve Malzeme Mühendisleri Odası, 2016.

[Dav01]   Davis, J.R.: Alloying: Understanding the Basics, ASM International, 2001.

[DIN10]   DIN EN ISO 6892-1: Metallic materials- Tensile testing - Part 1: Method of test at room temperature, 2010.

[DIN11]   DIN EN ISO 25239-4: Friction stir welding- Aluminum- Part 4: Specification and qualifications of welding procedures, 2011.

[Dog06]   DOGAN, S. 2006. AA 5754-H22 Alüminyum Alasımının Sürtünme Karıstırma Kaynağında Islem Parametrelerinin Mikro yapı ve Mekanik Özelliklere Etkileri. Yüksek Lisans Tezi. Osmangazi Üniversitesi Fen Bilimleri Enstitüsü, Eskisehir.

[Don01]   Dong, P.; Lu, F.; Hong, J.; Cao, Z.: Coupled thermomechanical analysis of friction stir welding process using simplified models. Science and Technology of Welding and Joining, 6/5, 2001.

[Eaa15]   The Aluminum Joining Manual, European Aluminum Association (EAA), p.3, 2015.

[Eaa17]   Aluminum in Commercial Vehicles Manual, European Aluminum Association (EAA), p.2, 2017.

[Ema17]   Emamian, S.; Awang, M.; Yusof, F.; Hussain, P.; Mehrpouya, M.; Kakooei, S.; Moayedfar, M.; Zafar, A.: A Review of Friction Stir Welding Pin Profile, Awang (Ed.) – 2nd International Conference on Mechanical, 2017.

[Gol15]   Golezani, A.S.; Barenji, R.V.; Heidarzadeh, A.; Pouraliakbar. H.: Elucidating of tool rotational speed in friction stir welding of 7020-T6 aluminum alloy. International Journal of Advanced Manufacturing Technology. 81:1155– 1164, 2015.

[Jat00]   Jata, K.V.; Sankaran K.K; Ruschau, J. J.: Friction-Stir Welding Effects on Microstructure and Fatigue of Aluminum Alloy 7050-T7451, Metallurgical and Materials Transactions A, Volume 31a, 2000.

[Jat01]   Jata, K.V.; Mahoney, M.W.; Mishra, R.S.; Semiatin, S.L.: Friction Stir Welding and Processing, 2001.

[Kah15]   Kah, P.; Rajan, R.; Martikainen, J.; Suoranta, R.: Investigation of weld defects in friction-stir welding and fusion welding of aluminum alloys, International Journal of Mechanical and Materials Engineering, 2015.

[Kas16]   Kasman, S.; Kahraman, F.; Aydin, A.: Sürtünme Karıştırma Kaynak Yöntemi ile Birleştirilmiş AA7075-T651 Alüminyum Alaşımlarının Farklı Karıştırıcı Pim Geometrilerinin Kaynak Performansına Etkisinin İncelenmesi, ISITES2016 Alanya/ Antalya – Turkey, 2016.

[Kau00]   Kaufman, G.: Introduction to Aluminum Alloys and Tempers, ASM International, 2000.

[Kha17]   Khan, N. Z.; Khan, Z. A.: Friction stir welding. Dissimilar aluminum alloys. Boca Raton: CRC Press Taylor & Francis Group, 2017.

[Kho08]   Khodir, S.A.; Shibayanagi, T.: Friction Stir Welding of Dissimilar AA2024 and AA7075 Aluminum Alloys. Materials Science and Engineering B, 148, pp.82-87, 2008.

[Kum12]   Kumbhar, N. T.; Bhanumurthy, K.: Friction Stir Welding ofAl 5052 with Al 6061 Alloys, Hindawi Publishing Corporation Journal of Metallurgy, 2012.

[Kum15]   Kumar, N.; Yuan, W.; Mishra R. S.: Friction Stir Welding of Dissimilar Alloys and Materials, Elsevier Inc., 2015.

[Kou87]   Kou, S.: Welding Metallurgy, John Wiley & Sons, p.10, 1987.

[Li13]   Li, J.Q.; Liu, H.J.: Effects of welding speed on microstructures and mechanical properties of AA2219-T6 welded by the reverse dual-rotation friction stir welding. International Journal of Advanced Manufacturing Technology. 68:2071–2083, 2013.

[Loh10]   Lohwasser, D.; Chen, Z.: Friction stir welding From basics to applications, Woodhead Publishing Limited, 2010

[Mal10]   Malyer, E.: Sürtünme Karıştırma Kaynağı ile Birleştirilen 5000 Serisi Alüminyum Alaşımlarında Kaynak Karametrelerinin Incelenmesi, Doktora Tezi, Uludag University, 2010

[Mat02]   Mathers, G.: The Welding of Aluminum and its Alloys, Woodhead Publishing Ltd., pp.5, 7-9, 2002.

[Mei13]   Meilinger, A.; Török, I.: The Importance of Friction Stir Welding Tool, Production Processes and Systems, Vol.6, No.1, pp. 25-34, 2013

[Mis05]   Mishra, R. S.; Ma, Z. Y.: Friction stir welding and processing. In Materials Science and Engineering:R.Reports 50(1-2), pp.1-78, 2005.

[Mis07]   Mishra, R. S.; Mahoney, M.W.: Friction Stir Welding and Processing, ASM International, 2007.

[Moh12]   Mohanty, H. K.; Mahapatra, M. M.; Kumar, P.; Biswas, P.; Mandal, N. R.: Effect of Tool Shoulder and Pin Probe Profiles on Friction Stirred Aluminum Welds — A Comparative Study. J. Marine. Sci. Appl. 11 (2), pp. 200–207, 2012.

[NN13]   N.N; https://www.azom.com/article.aspx?ArticleID=9107. AZO Materials, 10.07.2013.

[NN19]   N.N; http://www.astmsteel.com/product/h13-tool-steel-x40crmov5-1-skd61-hot-work-steel/. Retrieved on 30.06.2019.

[Ole06]   Olea, C. A. W.; Roldo, L.; dos Santos, J., F.; Strohaecker, T.R.: Friction stir welding of precipitate hardenable aluminum alloys: A review. IIW—Welding in the World. 50(11/12), pp.78–87, 2006.

[Pai09]   Paik, J. K.: Mechanical properties of friction stir welded aluminum alloys 5083 and 5383, International Journal of Naval Architecture and Ocean Engineering 1, pp. 39-49, 2009.

[Pan14]   Panneerselvam, K.; Lenin, K.: Joining of Nylon 6 Plate by Friction Stir Welding Process Using Threaded Pin Profile, Materials and Design 53 pp.302–307, 2014.

[Pee06]   Peel, M.; Steuwer, A.; Withers, P.J.: Dissimilar friction stir welds in AA5083-AA6082. Part II process effects on microstructure. Metallurgical and Materials Transactions A 37/7, pp. 2195–2206, 2006.

[Pod15]   Podržaj,P.; Jerman, B.; Klobčar, D.: Welding Defects At Friction Stir Welding, Metalurgija 54, pp.387-389, 2015.

[Pra13]   Prakash, P.; Jha, S. K.; Lal, S. P.: A Study of Process Parameters of Friction Stir Welded AA 6061 Aluminum Alloy. International Journal of Innovative Research in Science, Engineering and Technology Vol.2, Issue 6, 2013.

[Sak09]   Sakthivel, T.; Sengar, G. S.; Mukhopadhyay, J.: Effect of welding speed on microstructure and mechanical properties of friction-stir-welded aluminum. In Int J Adv Manuf Technol 43 (5-6), pp. 468–473, 2009.

[Sha16]   Shah, P. H.; Badheka, V.: An Experimental Investigation of Temperature Distribution and Joint Properties of Al 7075 T651 Friction Stir Welded Aluminum Alloys. In Procedia Technology 23, pp. 543–550, 2016.

[Son03]   Song, M.; Kovacevic, R.: A Coupled Heat-Transfer Model for Workpiece and Tool in Friction Stir Welding, 4th International Symposium on FSW, Park City, 2003.

[Su03]   Su, J. Q.; Nelson, T.W.; Mishra, R.; Mahoney, M.: Microstructural investigation of friction stir welded 7050-T651 aluminum. Acta Materialia. 51:713–729, 2003.

[Thr97]   Threadgill, P.: Friction stir welds in aluminum alloys: Preliminary microstructural assessment, TWI Bulletin, pp. 38:30–33, 1997.

[Ull17]   Ullegaddi, K.; Murthy, V.; Harsha, R. N.; Manjunatha: Friction Stir Welding Tool Design and Their Effect on Welding of AA-6082 T6. In Materials Today: Proceedings 4 (8), pp. 7962–7970, 2017.

[Qui12]   Quintino, L.; Miranda, R.; Dilthey, U.; Iordachescu, D.; Banasik, M.; Stano, S.

[Ven13]   Venkateswarlu, D.; Mandal, N. R.; Mahapatra, M. M.; Harsh, S. P.: Tool Design Effects for FSW of AA7039, Welding Journal vol. 92, pp.41-47

[Xue11]   Xue, P.; Ni, D.R.; Wang, D., Xiao; B.L.; Ma, Z.Y.: Effect of Friction Stir Welding Parameters on the Microstructure and Mechanical Properties of the Dissimilar Al-Cu Joints. Materials Science and Engineering, A, 528, pp. 4683-4689, 2011

[Yan07]   Yan, J. H.; Sutton, M. A.; Reynolds, A. P.: Processing and banding in AA2524 and AA2024 friction stir welding. Science and Technology of Welding and Joining, 12/5, pp.390–401, 2007.

[Yav97]   YAVUZ, N.: Alüminyum Alasımlarında Silisyumun Kaynak Dikisi Mekanik Özelliklerine Etkisinin Incelenmesi. Pamukkale Üniversitesi Mühendislik Fakültesi, Mühendislik Bilimleri Dergisi, Cilt 3 Sayı 3 s. 441-445, 1997

[Zha05]   Zhao, Y.; Lin, S.; Wu, L.; Qu, F.: The influence of pin geometry on bonding and mechanical properties in friction stir weld 2014 Al alloy. In Materials Letters 59 (23), pp. 2948–2952, 2005

[Zha12]   Zhang, Y., N.; Cao, X.; Larose, S.; Wanjara, P.: Review of tools for friction stir welding and processing, Canadian Metallurgical Quarterly Vol.51, 2012

[Wem03]   Weman, K.: Welding Processes Handbook, Woodhead Publishing Ltd., p.26, 2003.

8 List of Figures

9   List of Tables